Mineralia Slovaca, 42 (2010), 33 – 56
ISSN 0369-2086

Gold mineralization and associated alteration zones of the Biely vrch Au-porphyry deposit, Slovakia

PETER KODĚRA[1], JAROSLAV LEXA[2], ADRIAN BIROŇ[3] and JURAJ ŽITŇAN[1]

[1]Comenius University, Faculty of Natural Sciences, Department of Geology of Mineral Deposits, Mlynská dolina, 842 15 Bratislava, Slovakia; kodera@fns.uniba.sk, jzitnan@gmail.com
[2]Geological Institute, Slovak Academy of Sciences, Dúbravská cesta 9, 840 05 Bratislava, Slovakia; Jaroslav.Lexa@savba.sk
[3]Geological Institute, Slovak Academy of Sciences, Severná 5, 974 01 Banská Bystrica, Slovakia; biron@savbb.sk

Abstract

The Biely vrch deposit is a new economic Au-porphyry mineralization discovered in Slovakia. The deposit is located in the central zone of the Neogene Javorie stratovolcano, and shares many properties typical for Au-porphyry deposits. Parental intrusion of diorite to andesite porphyry and its andesitic volcanic host rocks are affected by extensive alteration, dominated by intermediate argillic (IA) alteration represented mostly by I-S, illite, chlorite, epidote and pyrite. It variably overprints earlier high-T K-silicate (K-feldspar, biotite, magnetite) and Ca-Na silicate (basic plagioclase, actinolite) alteration in deeper levels of the system, respectively. Propylitic alteration (illite-smectite, chlorite-smectite, chlorite, quartz, pyrite) represents outer zone of the system. Ledges of advanced argillic (AA) alteration (kaolinite, dickite, pyrophyllite, vuggy quartz) correspond to the youngest stage of alteration, probably related to younger intrusive event. Alterations are accompanied by hydrothermal-explosive breccias and by several generations of veinlets including the oldest early biotite-magnetite (EB-type) and quartz-biotite-magnetite veinlets (A-type) associated with K-silicate alteration, later widespread quartz veinlets often with banded texture, younger pyrite veinlets (± rare chalcopyrite, marcasite, galena, sphalerite, molybdenite) and coeval IA veinlets affiliated to IA alteration and the youngest carbonate-zeolite and AA veinlets. Gold grains are of high fineness (875 – 994) and occur in the vicinity of quartz veinlets, in altered rock with clays (illite, I-S), chlorite and K-feldspar, sometimes attached to sulphides or Fe-Ti minerals. Crystallization of quartz and precipitation of Au was influenced by fluid decompression in a shallow level of the system and reaction of Au-bearing fluids with favourably altered rocks. Acid fluids forming the AA type of alteration caused locally remobilization of gold and its increase in fineness.

Key words: Au-porphyry, gold, alteration, veinlets, geochemistry, Javorie stratovolcano, Western Carpathians

Introduction

Porphyry gold deposits are a relatively new type of porphyry-type deposits, becoming increasingly important in the world. Classical Au-porphyry deposits are located in the Maricunga belt in northern Chile (Vila and Sillitoe, 1991; Muntean and Einaudi, 2001), but reported examples are also known from Peru, Nevada and California (Seedorf et al., 2005). In addition, Turkish Au-porphyry deposit Kisladag belongs nowadays to largest gold deposits in Europe with 10.4 Moz Au (www.eldoradogold.com).

Despite the Central Slovakian Volcanic Field was known to host Cu-Au skarn-porphyry and porphyry type of deposit and occurrences for a long time (Burian and Smolka, 1982; Marsina et al., 1995; Konečný et al., 1977; Štohl et al., 1981, 1986), the Au-porphyry represents here a new type of ore mineralization. It was discovered recently by the EMED Mining, Ltd. on several localities in the Javorie and Štiavnica stratovolcanoes, however only Biely vrch deposit reaches economic accumulation of the gold ore (Hanes et al., 2010). It is the largest and best explored Au porphyry system with economic mineralization extending to a depth of at least 450 m. Initial Mineral Resource estimate totals 42 Mt at 0.8 g/t Au (www.emed-mining.com). Previous works leading to the discovery of the deposit are summarized by Hanes et al. (l. c.).

The Biely vrch deposit shares many properties typical for Au-porphyry deposits in general, including the lowest Cu/Au ratio within porphyry type deposits (<0.04 % Cu ppm Au at the Biely vrch locality) and association with diorite porphyry intrusions (Sillitoe, 2000; Seedorf et al., 2005). The main aim of this paper is to describe details

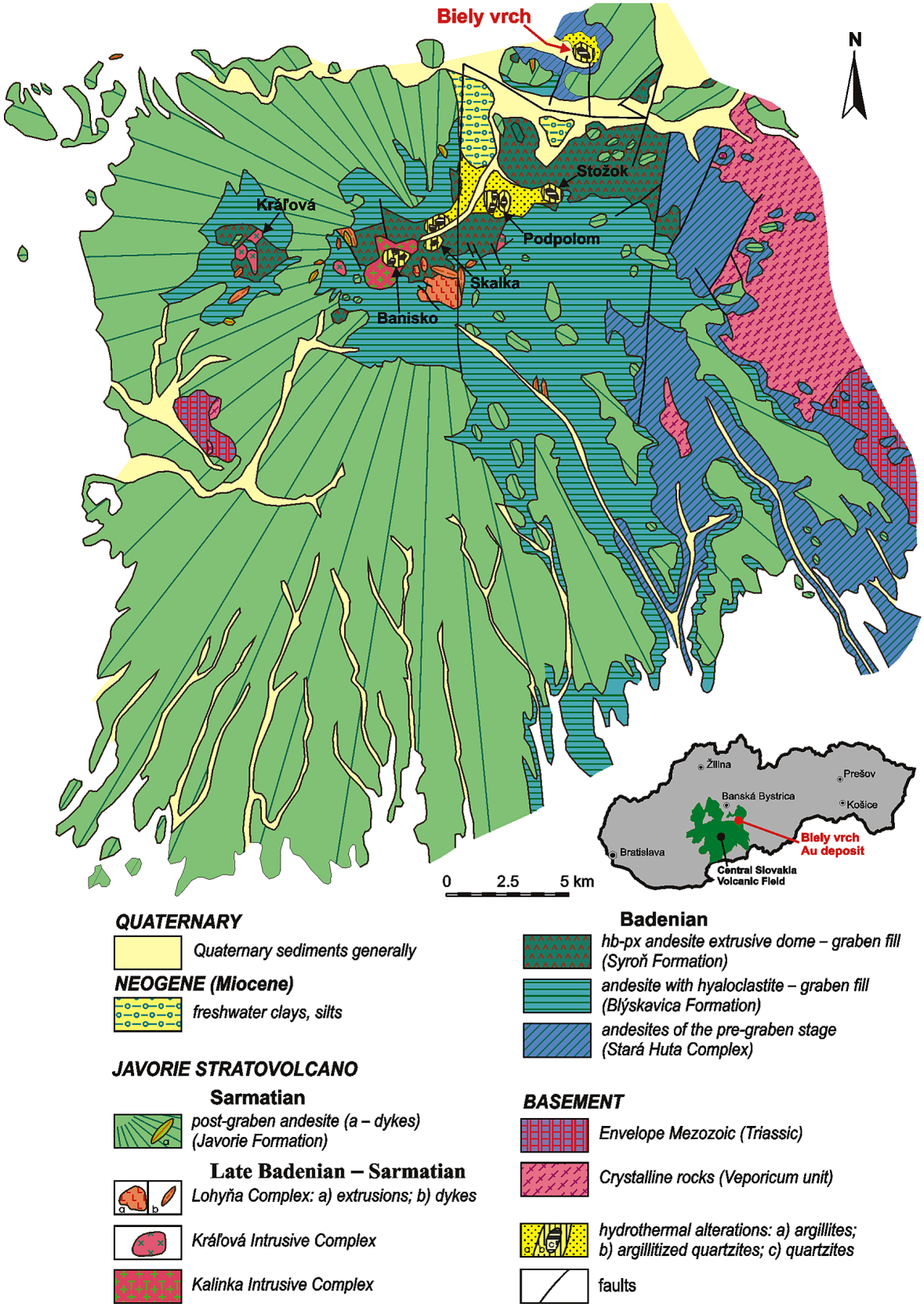

Fig. 1. Localization of the Biely vrch Au-porphyry deposit and other magmatic-hydrothermal systems in the structural scheme of the Javorie stratovolcano (modified after Konečný et al., 1998).

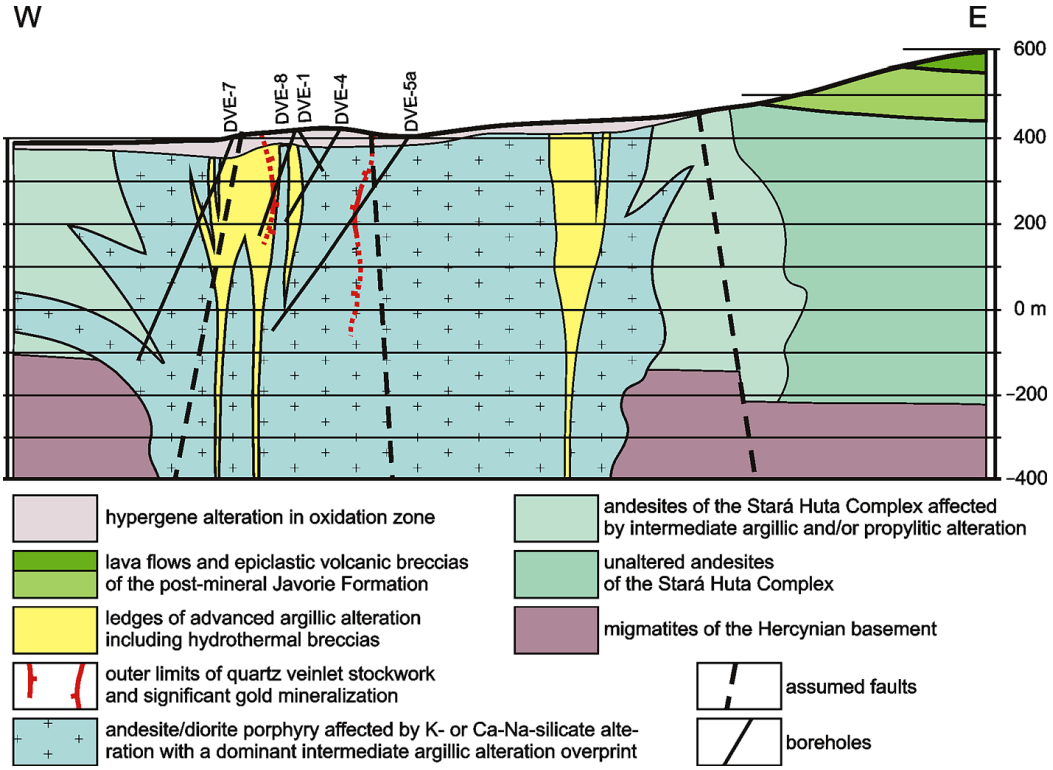

Fig. 2. Schematic geological section of the Biely vrch magmatic-hydrothermal system.

of alteration pattern and veinlets appearing at this deposit, including their typical mineral assemblages and relative age, as well as the main characteristics of associated Au mineralization.

Geological setting

The Biely vrch Au-porphyry deposit is hosted by the Middle Miocene Javorie andesite stratovolcano in the NE part of the Central Slovakia Volcanic Field (Fig. 1). The large compound stratovolcano involving a volcanotectonic graben and subvolcanic intrusive complex evolved in several stages of volcanic/magmatic activity (Konečný et al., 1998): (1) pre-graben stage – pyroxene and amphibole-pyroxene andesite effusive and explosive activity gave rise to a large andesite stratovolcano (Stará Huta Complex) formed by lava flows and subordinate pyroclastic breccias in the central zone and alternating lava flows with epiclastic breccias in the proximal zone; (1a) break in volcanic activity – erosion; (2) graben stage – subsidence of volcanotectonic graben in the central zone of the stratovolcano was accompanied first by effusive volcanic activity of olivine-bearing basalts, basaltic andesites and pyroxene andesites, that due to the limnic environment formed a complex of lava flows and hyaloclastite breccias (Blýskavica Formation), later by activity of differentiated pyroxene-hornblende andesites to dacites, forming extrusive domes with related coarse breccias and epiclastic volcanic breccias/conglomerates (Siroň Formation); (3) intrusive stage – emplacement of andesite porphyry, quartz-diorite porphyry and monsodiorite stocks (Kalinka and Kráľová intrusive complexes) into subsided complexes of the graben filling accompanied by the evolution of magmatic-hydrothermal systems (including the Biely vrch system); rare rhyodacite dykes (Lohyňa Complex) postdate porphyry intrusions and related mineralization; (3a) break in volcanic activity – erosion; (4) post-graben stage – pyroxene and amphibole-pyroxene andesite effusive and explosive volcanic activity gave rise to stratovolcanic complex of the Javorie Formation, dominantly effusive complex in the central zone passes outward into the complex of lava flows and coarse epiclastic volcanic breccias in the proximal zone and epiclastic volcanic breccias, conglomerates and sandstones in the distal zone.

Altogether 6 magmatic-hydrothermal systems are related to subvolcanic andesite and diorite porphyry intrusions of the Kráľová and Kalinka intrusive complexes in the central zone of the Javorie Stratovolcano (Fig. 1). The Biely vrch Au deposit is hosted by the northernmost system located in a relatively shallow NE part of the volcanotectonic graben. It is situated in the central part of the down-faulted block, with estimated depth of basement around 500 m (Konečný et al., 1988). The historical borehole DV-24 northwest of the prospect reached basement in the depth of 472 m (Mihaliková, 1985), while some of the recent boreholes have detected the presence of large pendants in various depths. Basement is represented by Hercynian tonalite and subordinate migmatite with frequent zones of shearing. Especially along shear zones they are affected by hydrothermal alteration related to the porphyry system.

Volcanic rocks that rest on the Hercynian basement in thickness around 500 m belong to the Stará Huta Complex (Fig. 2). They extend around parental intrusion of the magmatic-hydrothermal system. Massive pyroxene-

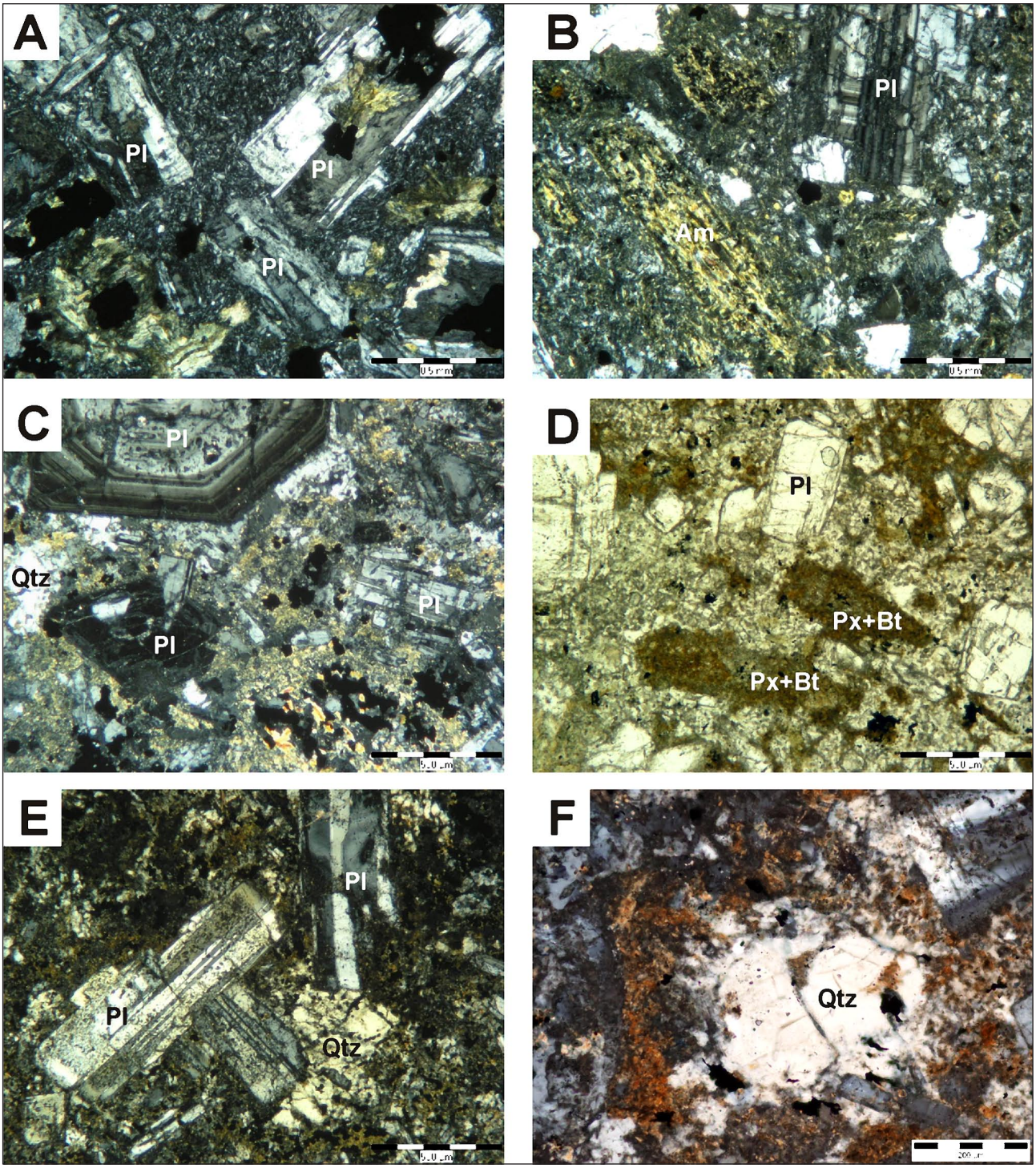

Fig. 3. Microphotographs of primary rocks of the Stará Huta Complex and diorite porphyry (parental intrusion): **A** – pyroxene andesite with phenocrysts of zonal plagioclase in pilotaxitic/trachytic groundmass (DVE-7/536.2 m, XN); **B** – biotite-amphibole-pyroxene andesite – altered amphibole next to a zonal plagioclase phenocryst in microlitic groundmass (DV-24/105.5 m, XN); **C** – zonal plagioclase phenocryst in holocrystalline groundmass with poikilitic quartz (DVE-5a/57.4 m, XN); **D** – pyroxene phenocrysts replaced by biotite in allotriomorphic granular groundmass (DVE-5a/42.5 m, IIN); **E** – "quartz eye" showing poikilitic relationship to plagioclase phenocrysts (DVE-5a/118.3 m, XN); **F** – "quartz eye" showing overgrowth during groundmass crystallization (DVE-5a/42.5 m, XN).

-amphibole, amphibole-pyroxene and pyroxene andesite lava flows alternate with block-lava type and/or hyaloclastite breccias (Konečný et al., 2002). Closer to the center the rocks are affected by argillic and propylitic/chloritic alteration that fades out with increasing distance.

The parental intrusion of the Biely vrch Au-porphyry deposit is situated in the central part of the magmatic--hydrothermal system (Fig. 2). It is hosted primarily by the rocks of the Stará Huta Complex and extends downward into rocks of the Hercynian basement. Extensive alteration obscures primary nature of rocks. Consequently, the form and petrography of the intrusion remain at least partially hypothetical. Variability in groundmass texture implies a probable transition from diorite porphyry in the central part of the intrusion to andesite porphyry close to contacts and in apophyses. As far as the form of the intrusion is concerned facts are rather scarce. We assume a stock-like form with deep roots (Fig. 2), but the extent of the stock could not be defined exactly enough and outer limits are set just by recognized andesites of the Stará Huta Complex. There are two pieces of evidence pointing to the presence of apophyses at the level of the Stará Huta Complex: (1) diorite porphyry makes up a sill in the interval 299.6 – ~390 m in the borehole DV-24 (Mihaliková, 1985; reinterpretation in Konečný et al., 2002); (2) occurrence of andesite among diorite porphyries in the borehole DVE-7 (536.2 m).

Rocks of the "post-mineralization" Javorie Formation build up upper parts of ridges south and east of the magmatic-hydrothermal system. They rest on eroded surface of altered and unaltered rocks of the Stará Huta Complex in thickness up to 100 m. Fine to coarse epiclastic volcanic breccias/conglomerates of pyroxene and amphibole-pyroxene andesites in the lower part of the formation are covered by amphibole-pyroxene andesite lava flows.

Methodology

Description of rocks, alteration patterns and mineralogy is based on macroscopic core observations, core logs and geochemistry data especially from boreholes DVE-1, DVE-4, DVE-5a, DVE-7 and DVE-8a along the E–W section of the deposit (Figs. 2 and 4), provided kindly by the EMED Slovakia, s. r. o., and published with their permission (for analytical details see Hanes et al., 2010 in this issue). The laboratory evaluation of samples also included transmitted and reflected light optical microscopy, XRD and microprobe analyses, including the cathodoluminiscence study. Analyses of gold presented below were performed at the State Geological Institute of Dionýz Štúr on the electron microprobe CAMECA SX 100.

Mineral abbreviations used in this paper: actinolite – Act, allanite – Aln, alunite – Alu, amphibole – Am, apatite – Ap, augelite – Agl, biotite – Bt, calcite – Cal, diaspore – Dsp, epidote – Ep, fluorite – Fl, galenite – Gn, chalcopyrite – Ccp, chlorite – Chl, illite – Ill, illite-smectite – I-S, ilmenite – Ilm, kaolinite – Kln, K-feldspar – Kfs, magnetite – Mag, marcasite – Mrc, molybdenite – Mo, plagioclase – Pl, pyrrhotite – Po, pyrite – Py, pyrophyllite – Prl, pyroxene – Px, quartz – Qtz, rutile – Rt, smectite – Sme, sphalerite – Sp, titanite – Ttn, woodhousite – Wod, zeolite – Zeo.

Primary rocks

Rocks hosting the Biely vrch Au-porphyry deposit are mostly altered beyond their recognition. Either they are metasomatites without any remnants of the former texture, or they show only obscured remnants of the porphyritic texture not allowing assignment of the rock to one of the primary rock types. Despite this fact, in several thin sections of less altered rocks we have managed to identify their original nature.

Andesites belong to the Stará Huta Complex and represent host rocks of the parental intrusion. Three types of andesite have been recognized in samples from outskirts of the deposit: (1) pyroxene andesite with pilotaxitic/trachytic groundmass (in DVE-7/536.2 m; Fig. 3A); (2) pyroxene andesites with microlitic groundmass (in DV-24/286.5 m, 432.7 m); (3) pyroxene-amphibole andesite with accessory biotite (or biotite-pyroxene-amphibole andesite) with microlitic groundmass (in DV-24/93.8 – 213.5 m; Fig. 3B).

Andesite/diorite porphyry parental intrusion does not seem to represent multiple emplacements. Observed variability in groundmass textures corresponds to variability in the cooling rate rather than to several phases of magma emplacement. No significant changes in phenocryst assemblage have been observed and alterations and their zoning represent a simple succession corresponding to the one act of magma emplacement. However, late stage ledges of advanced argillic alteration point to the emplacement of a new portion of magma in greater depth (see arguments in discussion). A rare post-mineralization dyke has been identified in the borehole DVE-41/453 to 456 m (Hanes et al., 2010).

The parental intrusion is represented by amphibole--pyroxene diorite porphyry with accessory biotite (Figs. 3C and 3D). A variety with fine-grained holocrystalline groundmass close to contacts and in apophyses may be termed as andesite porphyry. The phenocrysts assemblage is dominated by zonal plagioclase. Pyroxenes, subordinate amphibole and rare biotite make up mafic phenocrysts. Groundmass shows variability in grain-size (0.05 to 0.2 mm, 0.3 mm in the case of poikilitic quartz) as well as a slight variability in mineral composition. Its texture varies from allotriomorphic-granular, composed predominantly of quartz and K-feldspar, to hypidiomorphic-granular or even micropoikilitic with substantial presence of plagioclase (quartz makes poikilitic grains in that case).

In some parts of the diorite porphyry intrusion sporadic larger quartz grains have been observed that are usually termed as "quartz eyes" (Figs. 3E and 3F). They are formed by single or several quartz grains, showing sometimes slight undulosity. They post-date phenocrysts as they show features of poikilitic overgrowth in respect to zonal plagioclase (Fig. 3E). On the other hand, they show additional growth during the groundmass crystallization, or recrystallization (Fig. 3F). So, the "quartz eyes" are

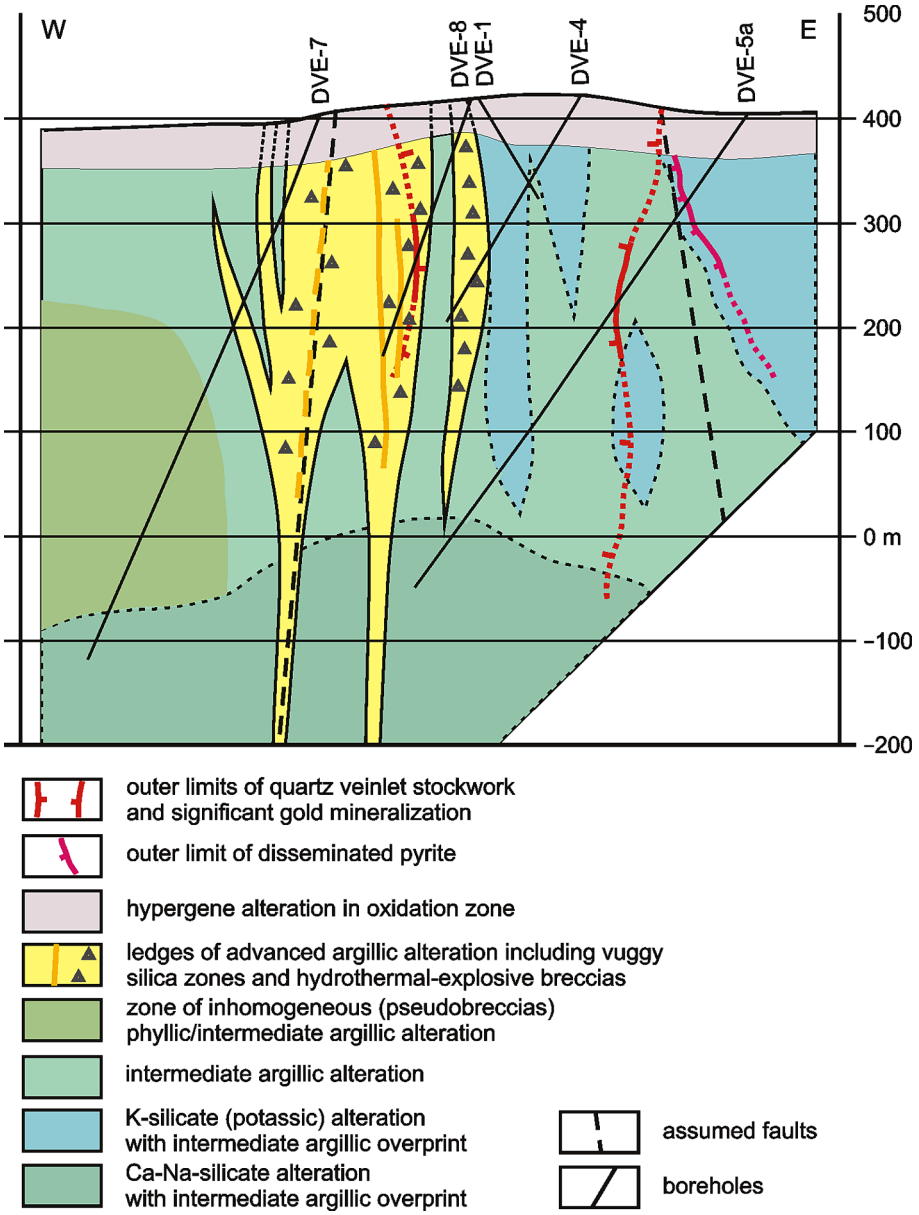

Fig. 4. Alteration pattern of the Biely vrch magmatic-hydrothermal system.

a late magmatic or early subsolidus feature. Vasyokova et al. (2008) relate quartz eyes to the process of in situ segregation of SiO_2- and H_2O-rich fluids.

Alterations and their succession

Parental intrusion of the Biely vrch Au-porphyry deposit and its host rocks are affected by intensive as well as extensive alteration. Most of the rocks are in reality metasomatites with no or limited extent of primary minerals and/or features. Alterations took place during several stages with changing PTX properties of fluids, resulting in overprinting of earlier mineral associations. Resulting assemblages of secondary minerals are very complex and mineral associations characteristic of individual alteration types were in practice difficult to determine. Coming from the environment of fresh rocks outside of the magmatic--hydrothermal system the following essential alteration zones could be recognized (Fig. 4): (1) outer zone of propylitic/chloritic alteration; (2) inner zone of intermediate argillic alteration, variably overprinting earlier higher temperature alteration types (K-silicate in the shallower level and Ca-Na-silicate in the deeper level of the system); (3) quartz veinlet stockwork locally accompanied by hydrothermal breccias in the center of the system – its extent corresponds roughly to the extent of significant gold mineralization and in that sense it represents the ore deposit itself; (4) younger ledges of advanced argillic alteration including hydrothermal-explosive breccias and zones of vuggy silica in their center.

Ca-Na-silicate alteration

This type of early high-temperature alteration occurs only in lowermost parts of deeper boreholes DVE-5a and DVE-7 (Fig. 4). It is represented by homogeneous plagioclase of intermediate to basic composition (An_{65} – An_{85}) replacing former zonal plagioclase phenocrysts (Figs. 5A and 5B) or occurring in newly-formed aggregates. Actinolite and magnetite are also characteristic minerals. Actinolite replaces former mafic phenocrysts (Fig. 5C) and shows a variable Fe/Mg ratio and Si-content. Frequent association of these minerals with biotite and K-feldspar points to a hybrid Ca-Na silicate/K-silicate alteration type (Sillitoe, 2000). Biotite and magnetite appear also as short irregular veinlets. Minerals of the Ca-Na-silicate alteration are variably accompanied by chlorite, illite, smectite and pyrite that represent an intermediate argillic alteration overprint. Its intensity increases in segments with a higher degree of fracturing and late stage carbonate veinlets.

Whole-rock geochemistry data show increased Ca and decreased K concentrations in deeper drillholes DVE-5a and DVE-7 starting from depth 420 m and 300 m, respectively (Fig. 6). Sodium content is not affected.

K-silicate alteration

Early high-temperature K-silicate type of alteration affected the upper part of the andesite/diorite porphyry stock above the zone of Ca-Na-silicate alteration (Fig. 4). However, due to a strong intermediate and/or advanced argillic overprint K-silicate mineral assemblages have been preserved only locally. Elsewhere the former K-silicate alteration mineral assemblage was replaced completely by mineral assemblages of the intermediate or advanced argillic type.

K-feldspar (orthoclase with 8 – 15 % albite component), Mg-rich biotite and magnetite are typical K-silicate alteration minerals. K-feldspar is replacing plagioclase phenocrysts (Figs. 5F and 5G) and forming irregular aggregates in groundmass, especially in the vicinity of biotite-magnetite-quartz veinlets. Biotite and magnetite replace former mafic phenocrysts (Figs. 3D and 5E) and groundmass (Fig. 5D) and occur in irregular aggregates and short irregular veinlets. Apatite, ilmenite, rutile, monasite and chalcopyrite appear as minor constituents. Alteration of higher intensity resulted in the origin of aggregates and veinlets of secondary minerals that entirely destroy the former porphyritic texture.

K-silicate alteration mineral assemblage is always associated with chloritic and/or intermediate argillic overprint of variable intensity, represented at least by chlorite with magnetite (Fig. 5F). More often illite, illite/smectite, smectite, apatite, rutile, pyrite, quartz and carbonate are also present.

Geochemical data demonstrate that all studied drillholes above the zone of Ca-Na alteration show roughly similar potassium content (~2 – 4 % K), except of sections strongly affected by advanced argillic alteration (Fig. 6).

Chloritic alteration

Chloritic alteration is not an individually recognized alteration type in porphyry systems, as the chlorite-rich assemblages are often described as parts of phyllic or intermediate argillic types of alteration. Also in the case of the Biely vrch magmatic-hydrothermal system chlorite occurs most often associated with the intermediate argillic mineral assemblage. However, locally chlorite, interlayered chlorite/smectite and magnetite replace former mafic minerals or secondary biotite, without other minerals of the intermediate argillic mineral assemblage (Fig. 5H). Rare chlorite and/or chlorite-magnetite veinlets have been observed too. Sporadic chloritic alteration represents probably a transitional stage between the K-silicate and intermediate argillic alteration stages.

Intermediate argillic alteration

Intermediate argillic (IA) alteration is the most widespread type of alteration, overprinting partially or completely mineral assemblages of the Ca-Na- and K-silicate alterations. Intensity of the alteration is highly variable on the meter scale. Higher intensity of alteration associates usually with a higher density of contemporaneous veining and/or increased tectonic fracturing of the parental porphyry. Quartz, chlorite, chlorite/smectite, illite, illite/smectite, smectite, pyrite, chalcopyrite, marcasite, apatite, rutile, ilmenite and carbonate are characteristic minerals. Minor magnetite, sphalerite, galena, K-feldspar poor in albite component and/or kaolinite might be present too (Figs. 7B and 7D). At lower intensity of alteration secondary minerals respect former minerals and porphyritic texture of the host rock is preserved as phantoms (Fig. 7D). At higher intensity of alteration secondary minerals loose the former mineral shape and instead they form irregular aggregates with no relationship to former porphyritic texture (Figs. 7B and 7C). There are several veinlet types that accompany intermediate argillic alteration: quartz veinlets with chlorite, clay minerals and/or pyrite accompanied by argillic halos, pyrite veinlets and intermediate argillic veinlets with chlorite and/or clay minerals (described below).

Mineral assemblage of intermediate argillic alteration is usually not uniform and its variability is expressed by changing colors (Fig. 7A). Inhomogeneous rocks or even pseudobreccias composed of pale and dark greenish domains are quite frequent. For instance, in large parts of boreholes DVE-5a (304 – 319 m, 376 – 406 m, 448 – 475 m) and DVE-7 (from 330 m downward) inhomogeneously altered parental diorite porphyry passes into breccia-like texture of dark "fragments" in gray, pale or even almost white "matrix" (Figs. 7E and 7F). At few places "fragments" show angularity and the rock might be interpreted as altered hydrothermal-explosive breccia or volcaniclastic rock. However, the "fragments" are mostly round, elliptical, irregular or even amoeba-like, showing shapes that could not result from brecciation or volcanic/sedimentary processes (Figs. 7E and 7F). No textures characteristic of volcaniclastic rocks (bedding, sorting, large fragments, porous fragments etc.) have been observed. However,

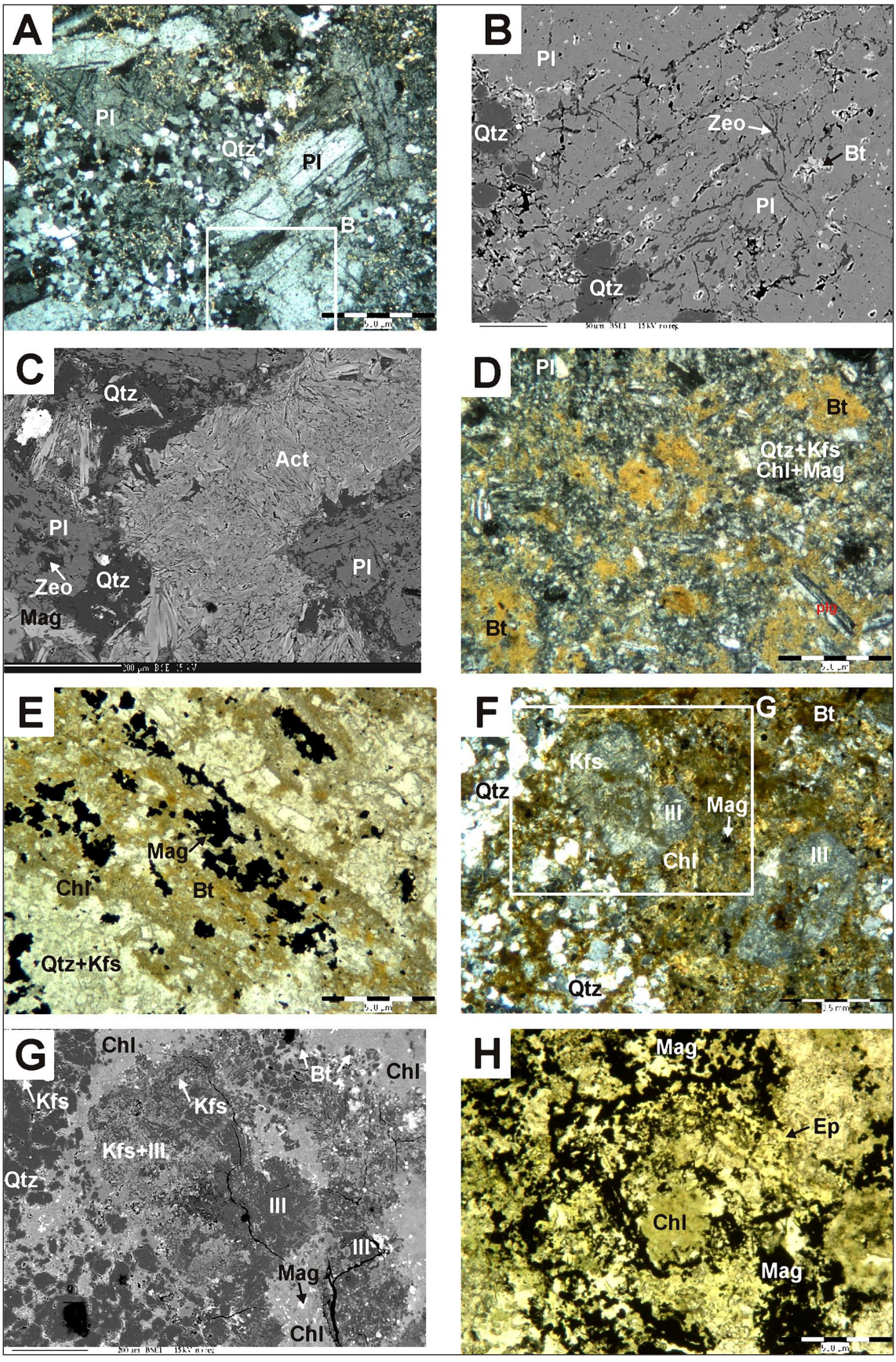

Fig. 5. Microphotographs of Ca-Na silicate, K-silicate and chloritic alteration at the Biely vrch magmatic-hydrothermal system: **A** – plagioclase phenocrysts replaced by homogeneous basic plagioclase (DVE-5a/495.5 m, XN); **B** – BSE image of detail from A showing homogeneous plagioclase (An_{85}) replacing former zonal phenocryst; **C** – homogeneous secondary plagioclase (An_{65}) with actinolite aggregate and quartz (DVE-7/567.0 m, BSE image); **D** – secondary biotite (brown) replacing mafic minerals and groundmass of diorite porphyry (DVE-7/424.4 m, XN); **E** – secondary biotite and magnetite replacing amphibole phenocryst (DVE-5a/57.4 m, IIN); **F** – K-silicate assemblage (Kfs, Bt, Mag) affected by chloritic/intermediate argillic alteration (chlorite, magnetite, illite, Na-rich, K-feldspar, quartz) (DVE-1/58.5 m, XN); **G** – BSE image – detail of the picture F; **H** – aggregate of chlorite, magnetite and minor epidote replacing former matic minerals (DVE-5a/314.3 m, IIN).

the nature of pseudobreccias in the borehole DVE-5a is different from those in the borehole DVE-7. In the borehole DVE-5a in dark domains ("fragments") the porphyry is replaced by epidote, chlorite, zeolite, smectite and magnetite and in pale domains ("matrix") the quartz and K-feldspar dominate over minor chlorite, illite and magnetite/pyrite. In the borehole DVE-7 in dark domains the porphyry is affected by intermediate argillic alteration with Mg-rich chlorite, smectite, carbonate, zeolite and pyrite as secondary minerals (Fig. 7H). Pyrite and pyrrhotite accumulate also at

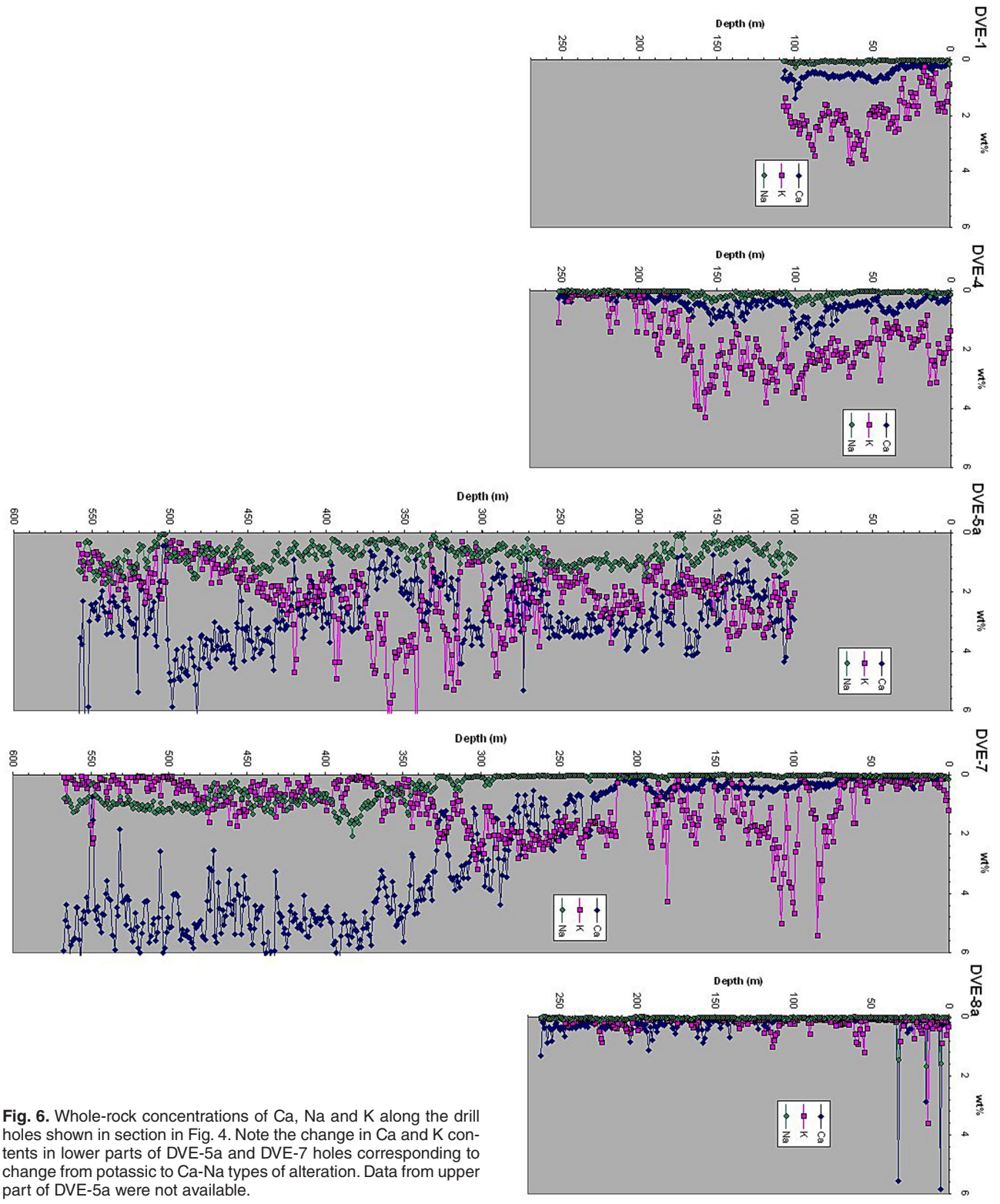

Fig. 6. Whole-rock concentrations of Ca, Na and K along the drill holes shown in section in Fig. 4. Note the change in Ca and K contents in lower parts of DVE-5a and DVE-7 holes corresponding to change from potassic to Ca-Na types of alteration. Data from upper part of DVE-5a were not available.

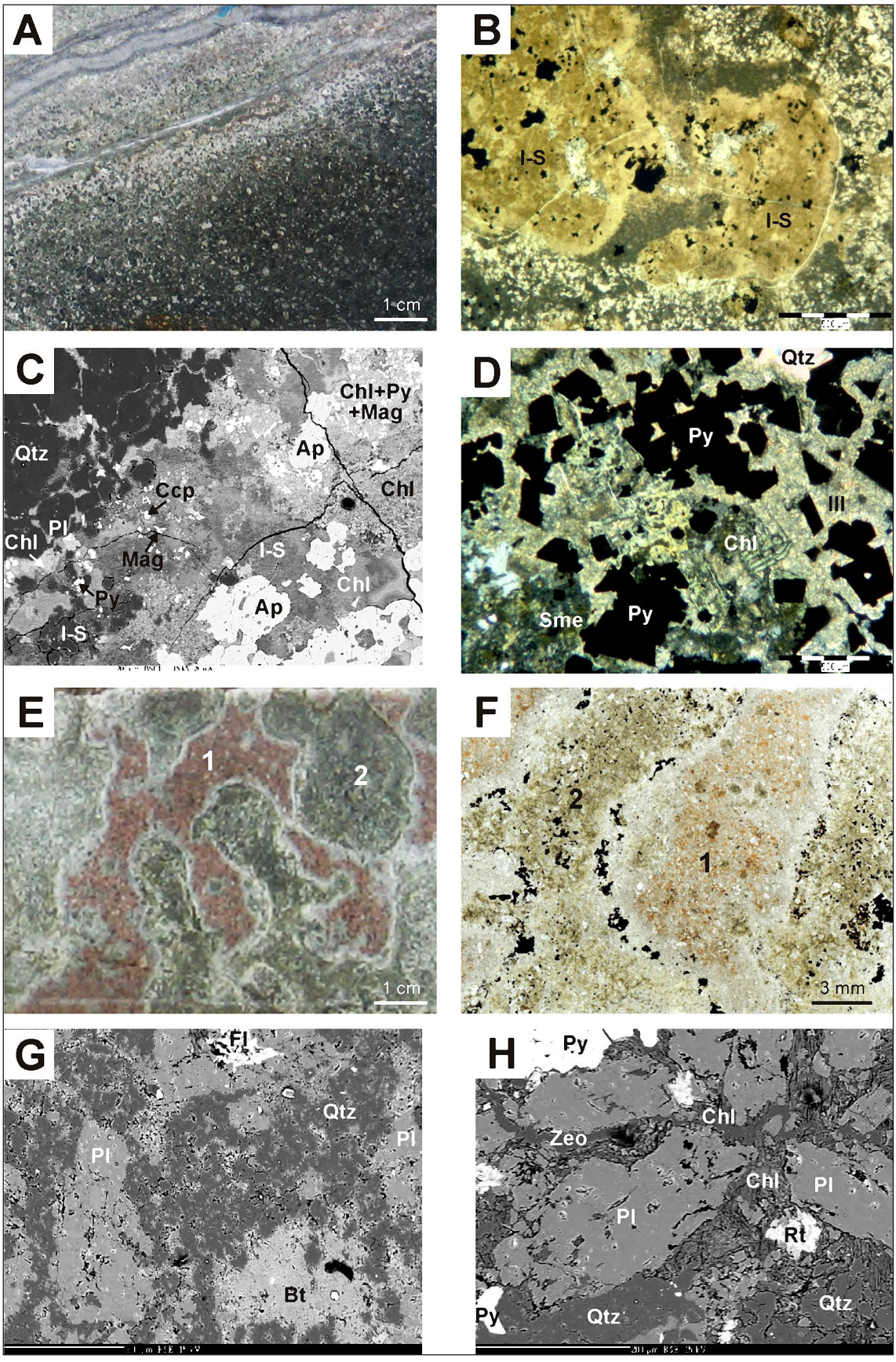

Fig. 7. Microphotographs of intermediate argillic alteration and associated pseudobreccias at the Biely vrch magmatic-hydrothermal system: **A** – porphyry affected by intermediate argillic alteration – note alteration halo next to veinlets (DVE-5a/180.7 m); **B** – aggregate of illite/smectite and pyrite replacing a former mafic phenocryst (DVE-5a/143.7 m, IIN); **C** – assemblage of intermediate argillic alteration minerals next to a quartz veinlet (DVE-4a/140.3 m, BSE image); **D** – aggregate of chlorite, smectite, illite and pyrite replacing former mafic phenocrysts (DVE-5a/90.5 m, XN); **E** – pseudobreccias formed of pale brownish domains (1) and dark greenish domains (2) – their shape excludes origin due to brecciation (DVE-7/424.4 m); **F** – two types of domains in thin section, note reaction rim with pyrite and pyrrhotite and absence of Fe-containing minerals next to it in the pale domain (DVE-7/424.4 m); **G** – BSE image of the pale domain 1; **H** – BSE image of the dark domain 2.

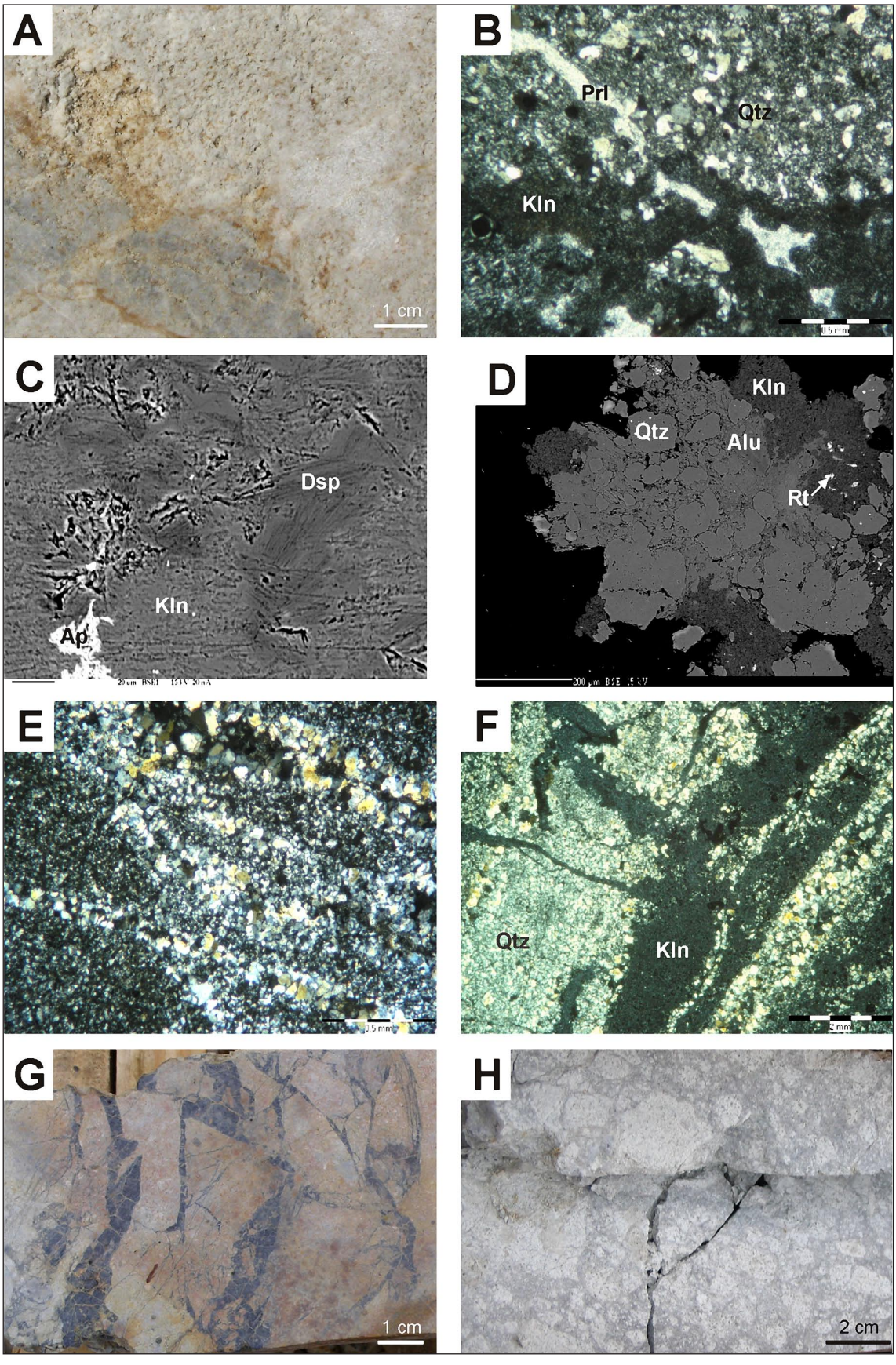

Fig. 8. Microphotographs of advanced argillic alteration and silicification at the Biely vrch magmatic-hydrothermal system: **A** – residual vuggy silica with alunite and pyrophyllite next to an older quartz vein (DVE-8a/224.0 m); **B** – quartz-kaolinite-pyrophyllite assemblage (DVE-6/217.1 m, XN); **C** – aggregate of kaolinite and diaspore with minor apatite (DVE-4/206.7 m, BSE image); **D** – kaolinite, alunite and rutile filling spaces among quartz grains in heavily silicified and argillized rock (DVE-8a/206.7 m, BSE image); **E** – silicification in association with a set of quartz veinlets in rock affected by intermediate argillic alteration (DVE-1/106.5 m, XN); **F** – silicification in association with kaolinite veinlets in rock affected by advanced argillic alteration (DVE-8a/43.7 m, XN); **G** – hydrothermal breccia associated with grey quartz veinlets (DVE-4/48.0 m); **H** – hydrothermal-explosive breccia with fragments of kaolinitic argillite (DVE-6/170.4 m).

the contact with pale domains as a reaction rim (Fig. 7F). Pale to brownish domains show earlier Na-Ca silicate and potassic alteration (homogenized basic plagioclase, biotite, magnetite; Fig. 7G) and later recrystallization with quartz and minor illite. The inhomogeneous to breccia-like texture is probably a result of variable alteration of the intermediate argillic type overprinting earlier Na-Ca/K-silicate alterations, perhaps due to incomplete replacement or less likely due to heterogenization of fluid or mixing of two types of fluids with contrasting properties.

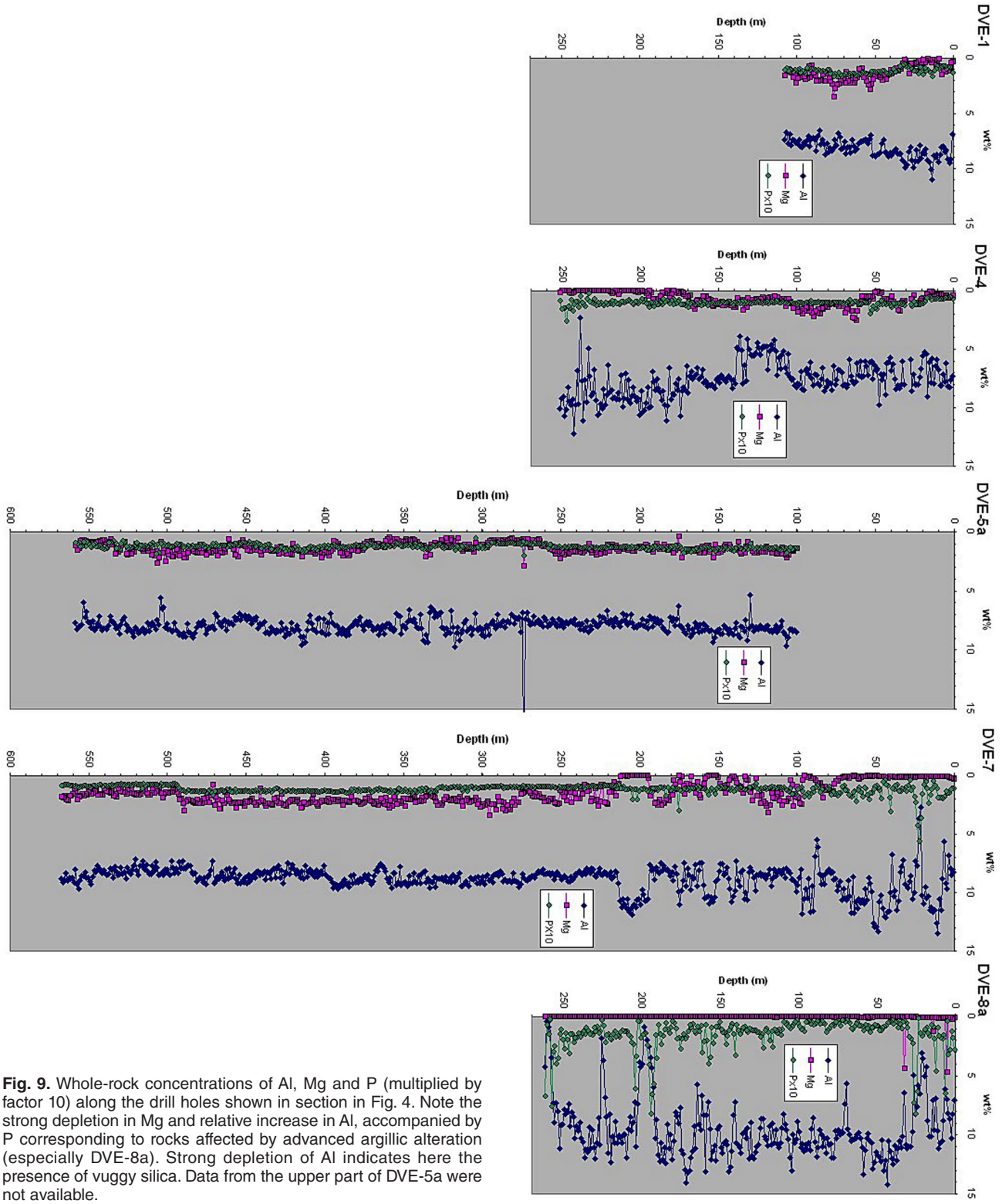

Fig. 9. Whole-rock concentrations of Al, Mg and P (multiplied by factor 10) along the drill holes shown in section in Fig. 4. Note the strong depletion in Mg and relative increase in Al, accompanied by P corresponding to rocks affected by advanced argillic alteration (especially DVE-8a). Strong depletion of Al indicates here the presence of vuggy silica. Data from the upper part of DVE-5a were not available.

As the Au porphyry systems are generally relatively depleted in sulphur, the quartz-sericite-pyrite (phyllic) alteration is usually not described from this type of deposits as an individual type of alteration (e.g. Muntean et al., 2001). However, zones enriched in pyrite/pyrrhotite exist on the Biely vrch deposit in its W part, as proven by some drill holes and an IP anomaly (Hanes et al., 2010). The increased amount of sulphur in this part of the system is also documented by whole-rock geochemistry data from the drill hole DVE-7 (Fig. 10), in some parts exceeding

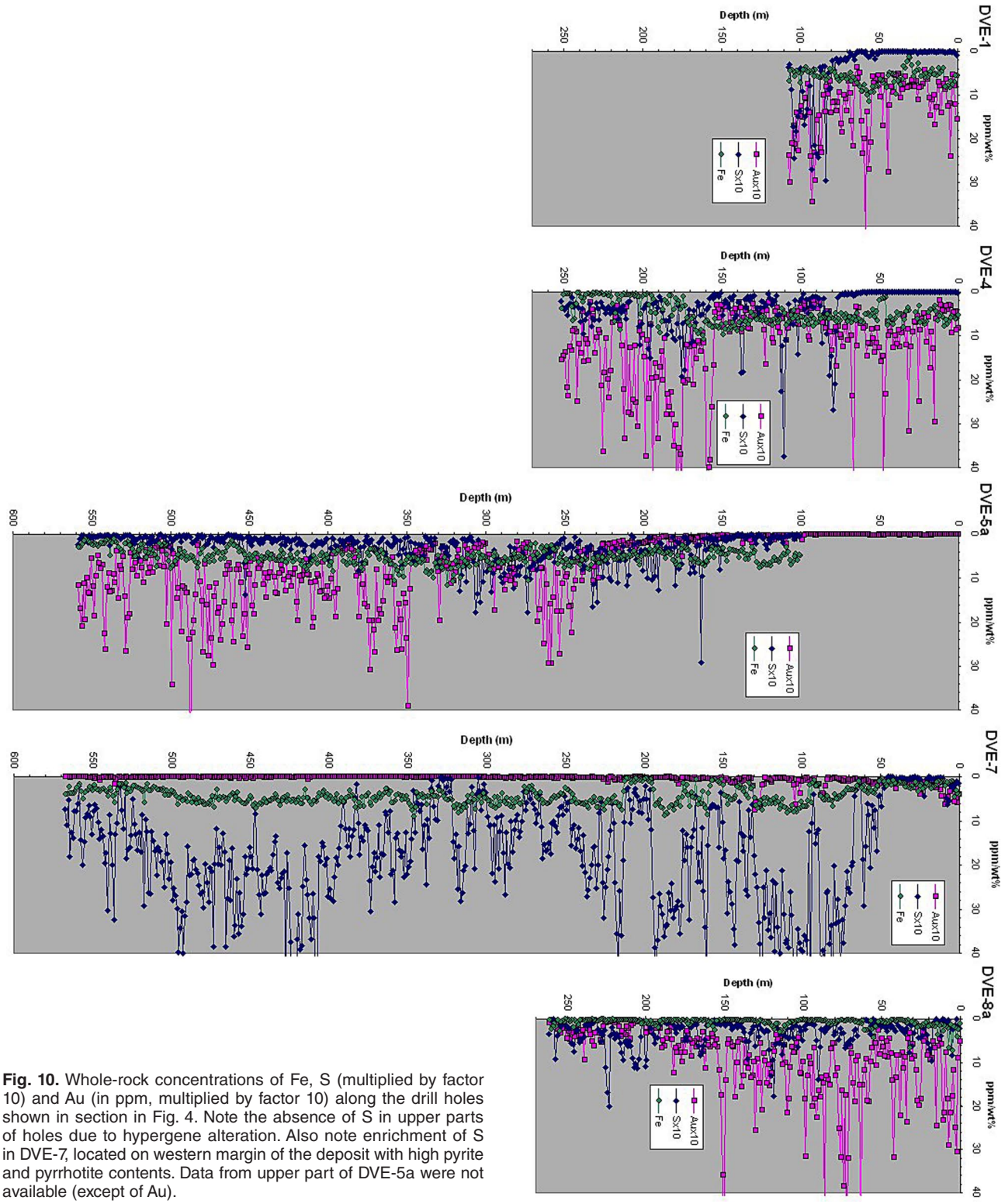

Fig. 10. Whole-rock concentrations of Fe, S (multiplied by factor 10) and Au (in ppm, multiplied by factor 10) along the drill holes shown in section in Fig. 4. Note the absence of S in upper parts of holes due to hypergene alteration. Also note enrichment of S in DVE-7, located on western margin of the deposit with high pyrite and pyrrhotite contents. Data from upper part of DVE-5a were not available (except of Au).

4 wt.% of S. However, it is not accompanied by an increase in Fe content, which has just changed from its oxidized to reduced form (i.e. magnetite to pyrrhotite/pyrite). In detail, this part of the deposit is represented by inhomogeneous intermediate argillic alteration (pseudobreccias with pyrite/pyrrhotite rims), described above.

Propylitic alteration

Propylitic alteration has been observed only in andesites from the externally situated borehole DV-24. Their porphyritic texture is well preserved. Plagioclase phenocrysts are either unaltered or replaced by a clay mineral (smectite?). Mafic phenocrysts are replaced by chlorite ± sericite and pyrite. Groundmass is recrystallized to fine aggregate of quartz, chlorite, interlayered chlorite/smectite and illite/smectite, pyrite and minor carbonate with rare pyrite and quartz-pyrite veinlets. Compared to typical propylitic mineral assemblages (e.g. Seedorf et al., 2005) the alteration is not complete – albite, epidote and carbonate are mostly missing. Consequently, the alteration of andesites in this borehole shows some affinity to the chloritic and/or intermediate argillic types of alteration.

Advanced argillic alteration

Advanced argillic alteration at the Biely vrch deposit forms two broad zones at the surface, several hundred meters long. These zones are structurally controlled, almost vertical (ledges), wedging out with increasing depth, where they are represented just by narrow zones decimeters to a few meters thick. Alteration overprints earlier alteration types described above (Fig. 4). In thicker ledges the hydrothermal-explosive breccias often occur, while in their center there is sometimes present a narrow zone of vuggy silica (Fig. 8A) resulting from leaching by fluids with the lowest pH. Based on XRD and microprobe analyses the mineral assemblage of the advanced argillic alteration includes kaolinite and/or dickite, pyrophyllite, alunite, diaspore, andalusite, augelite, dumortierite, millosevichite, topaz, rutile/leucoxene and a number of various unidentified Al-P-S-phases (Figs. 8B to 8D). Quartz, pyrophyllite, dickite, kaolinite and/or pyrite appear also as a matrix of hydrothermal-explosive breccias and veinlets.

The presence of advanced argillic alteration is clearly documented in the geochemistry pattern of the studied drill holes, especially the DVE-8a, which was running in rock strongly affected by this type of alteration. Typically, most major elements (Ca, Na, Mg, K and Fe) are strongly depleted, while aluminum content is relatively increased (Figs. 6, 9 and 10). In some narrow zones in DVE-8a even Al is strongly depleted, which indicates the presence of zones with residual vuggy silica (centered around 200 m, 228 m, 260 m). These zones apparently mark the location of faults introducing low pH fluids. In addition, the presence of phosphorus-bearing minerals accompanying this type of alteration corresponds to increased P contents, especially along zones with vuggy silica.

Silicification

Silicification does not represent an independent alteration type. It always associates with intermediate argillic or advanced argillic alterations. As a rule it occurs in surroundings of quartz veinlets (Fig. 8E) and associates with kaolinite/pyrophyllite veinlets (Fig. 8F). Typical are tile-like pattern of quartz grains and variability in grain size. At a low degree of silicification quartz only appears, forming discrete aggregates among other alteration minerals.

Hypergene alteration

Hypergene alteration corresponding to the extent of the oxidation zone is thanks to the presence of pyrite, magnetite and other easily altered minerals strong and deeply-reaching. Intense chemical weathering resulted in clay

Tab. 1
Summary of veinlet types at the Biely vrch deposit and their succession

	Bt-Mt-Qtz (EB-type, A-type)	Quartz	Pyrite (sulphide)	Intermediate argillic	Carbonate-zeolite	Advanced argillic
Major minerals	biotite, magnetite, quartz	quartz	pyrite	illite-smectite, illite, chlorite	calcite, zeolites	kaolinite, pyrophyllite
Minor minerals	K-feldspar, apatite	magnetite, chalcopyrite, pyrite, gold	chalcopyrite galena, sphalerite, tetrahedrite, pyrrhotite, Fe-Ti oxides	epidote, apatite Fe-Ti oxides, pyrite, chalcopyrite, molybdenite, tourmaline, xenotime, allanite, calcite, zeolite	chlorite, epidote, marcasite, pyrite, K-feldspar, apatite, illite-smectite, Fe-Ti oxides, tourmaline, allanite	dickite, alunite, woodhousite, augelite, pyrite, rutile
Associated alteration	potassic	intermediate argillic?	intermediate argillic	intermediate argillic	propylitic?	advanced argillic
Succession	1	2	3a	3b	4	5

and limonite rich regolith, whose thickness varies between 7 and 20 m on the top of the Biely vrch hill and its slopes (eluvial and deluvial deposits) and reaches down to 37 m in morphological depressions surrounding the Biely vrch (prolluvial deposits). Hypergene alteration extends from the surface down to the depth 30 – 50 m, in the central zone to about 120 m (Hanes et al., 2010). Pyrite and magnetite are completely or partially oxidized, other minerals with exception of quartz are affected variably by bleaching and kaolinization. Limonite occurs as pigment, aggregates and in veinlets (Fig. 12d). According to geochemical data the hypergene alteration is clearly demonstrated by complete removal of S and variably by depletion in K, Na, Ca, Mg contents of altered rocks (Fig. 10).

Hydrothermal-explosive breccias

Several types of hydrothermal-explosive breccias have been observed in the deposit. They are associated either locally with the origin of quartz veinlets (Fig. 8G), with intermediate argillic alteration, or most often with the late stage advanced argillic ledges (Fig. 8H). Rock fragments are usually cemented by argillized rock flour and/or vein-type material. Open spaces in brecciated rocks are sometimes filled with young carbonate-zeolite veinlets (outside the AA ledges). Breccias are mostly the result of mechanical disintegration due to hydrothermal-explosive processes that represent an extreme case of hydraulic fracturing with involvement of expanding vapor due to suddenly lowered pressure. Further studies are required to understand their nature (magmatic-hydrothermal vs. hydrothermal-explosive), succession, association with alteration types and relationship to mineralization.

Vein types and their succession

Altered rocks at the Biely vrch porphyry deposit contain several generations of veinlets of variable relative age (Tab. 1). Most of them are closely associated with the alteration patterns presented above, containing similar mineral assemblages.

Biotite-magnetite-quartz veinlets (EB- and A-types)

The oldest type of veinlets associates with K-silicate alteration and is represented by biotite, magnetite and quartz, rarely also K-feldspar (Figs. 11A, 12A and 12B). Generally, these veinlets are quite rare, but they were found in several boreholes in various depths (42 to 488 m). They are always quite narrow, mostly < 0.2 mm in diameter, rarely up to 0.5 mm. Typically, they are short, irregular in shape and lack internal symmetry. Sometimes, only magnetite is present forming short asymmetric veinlets, rarely accompanied by K-feldspar. Biotite-magnetite veinlets occasionally contain apatite and K-feldspar in their central parts, representing later stage of mineralization (Fig. 12A). If present, quartz is always older than biotite.

Biotite-magnetite-quartz bearing veinlets are found only in rocks affected by pervasive potassic alteration. They are always older than all other types of quartz veinlets and carbonate-zeolite veinlets (Fig. 11G). Based on their appearance, mineral content, relative age and association with potassic alteration they can be classified as EB--type and A-type of veinlets, based on the terminology of Gustafson and Hunt (1975) and Gustafson and Quiroga (1995), widely used in current literature. EB-type veinlets are defined as irregular streaky veinlets of biotite alone or with magnetite. A-type veinlets are defined as sugary, mostly discontinuous quartz veinlets with biotite, magnetite and/or chalcopyrite (Sillitoe, 2000; Muntean and Einaudi, 2001; Seedorf et al., 2005). Typically, these veinlets either have no alteration halos or halos with K-feldspar and/or biotite.

Quartz veinlets

Quartz veinlets are the most common type of veinlets at the deposit, forming a distinct stockwork zone within the porphyry intrusion ~500 x 300 m in diameter, roughly corresponding to the extent of gold mineralization. The zone with quartz veinlets starts from the surface down to at least ~450 m of depth, which is the lowermost explored part of the deposit. Quartz veinlets are younger then A- and EB-types of veinlets but older than various other types of veinlets.

Several generations of quartz veinlets have been recognized with clear crosscutting relationships of at least 3 generations in some samples (Fig. 11C). Their average thickness is about 0.2 – 0.5 cm, but some of them reach up to 1.5 cm. Veinlets are of grey to white colours, while some grey veinlets show clear banding. Banded quartz veinlets are younger than non-banded ones (Fig. 11C). Banding of quartz usually results from the high content of vapor-rich fluid inclusions and locally also from micrometer--sized magnetite and rare chalcopyrite and pyrite grains (Figs. 12C and 12E). Dark bands locally show botryoidal texture that is continuous along quartz veinlets (Fig. 12C), suggesting that the quartz recrystallized from silica gel (Ramdohr, 1980; Muntean and Einaudi, 2000). Botryoidal texture occurs either in the entire thickness of veinlets, or only in some bands, located in their central part, or on their margins. In some cases, the former botryoidal texture is completely destroyed by recrystallization, but the former texture can be still recognized by continuous bands of vapor-rich inclusions that do not respect quartz grains boundaries (Fig. 12D).

Central part of some quartz veinlets is filled by various later-stage minerals, elsewhere forming individual younger veinlets. They include: sulphides – mostly pyrite and chalcopyrite (Fig. 12G), variably also with marcasite, Fe-Ti oxides, galena, sphalerite (Fig. 12H); clay minerals (Figs. 13C and 13D) – mostly illite-smectite and/or chlorite, variably also with apatite, epidote, K-feldspar, tourmaline, xenotime; calcite and zeolite (Fig. 12G). These minerals either occur disseminated in cavities among individual quartz grains, in discontinuous clusters or in individual bands within the quartz veinlets (Fig. 12G). Quartz veinlets are spatially associated with increased concentrations of

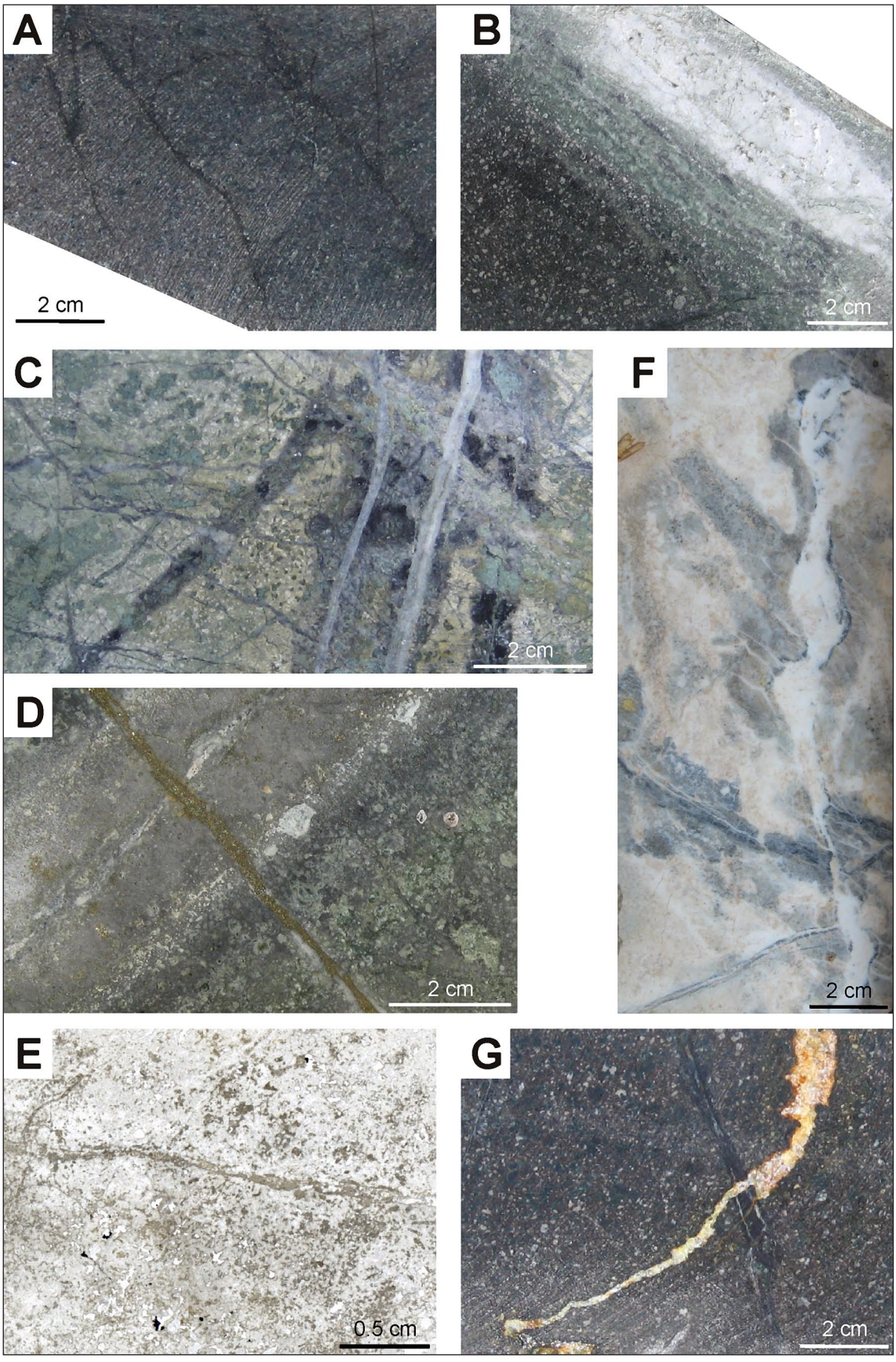

Fig. 11. Typical veinlet types at the Biely vrch deposit. **A** – biotite-magnetite veinlets (EB-type) hosted by altered diorite porphyry, affected by potassic and intermediate argillic alteration (DVE-5a/42.5); **B** – thick cluster of hydrothermal quartz in altered diorite porphyry, interpreted as xenolith of metamorphic hydrothermal quartz from the Hercynian crystalline basement, overgrown by porphyry-related hydrothermal quartz (DVE-5a/104.6); **C** – several generations of quartz veinlets in heavily silicified and argillized porphyritic rock (DVE-5a/455.2); **D** – pyrite ± quartz veinlet in argillized and silicified porphyritic rock (DVE-11/394.4); **E** – illite veinlet and aggregates in silicified and argillized porphyritic rock (DVE-1/91.5); **F** – kaolinite veinlet (white) cutting quartz veinlets in rock heavily altered by advanced argillic alteration (DVE-8a/43.7); **G** – carbonate-zeolite veinlet cutting A-type veinlet in altered diorite porphyry (DVE-5a/56.8).

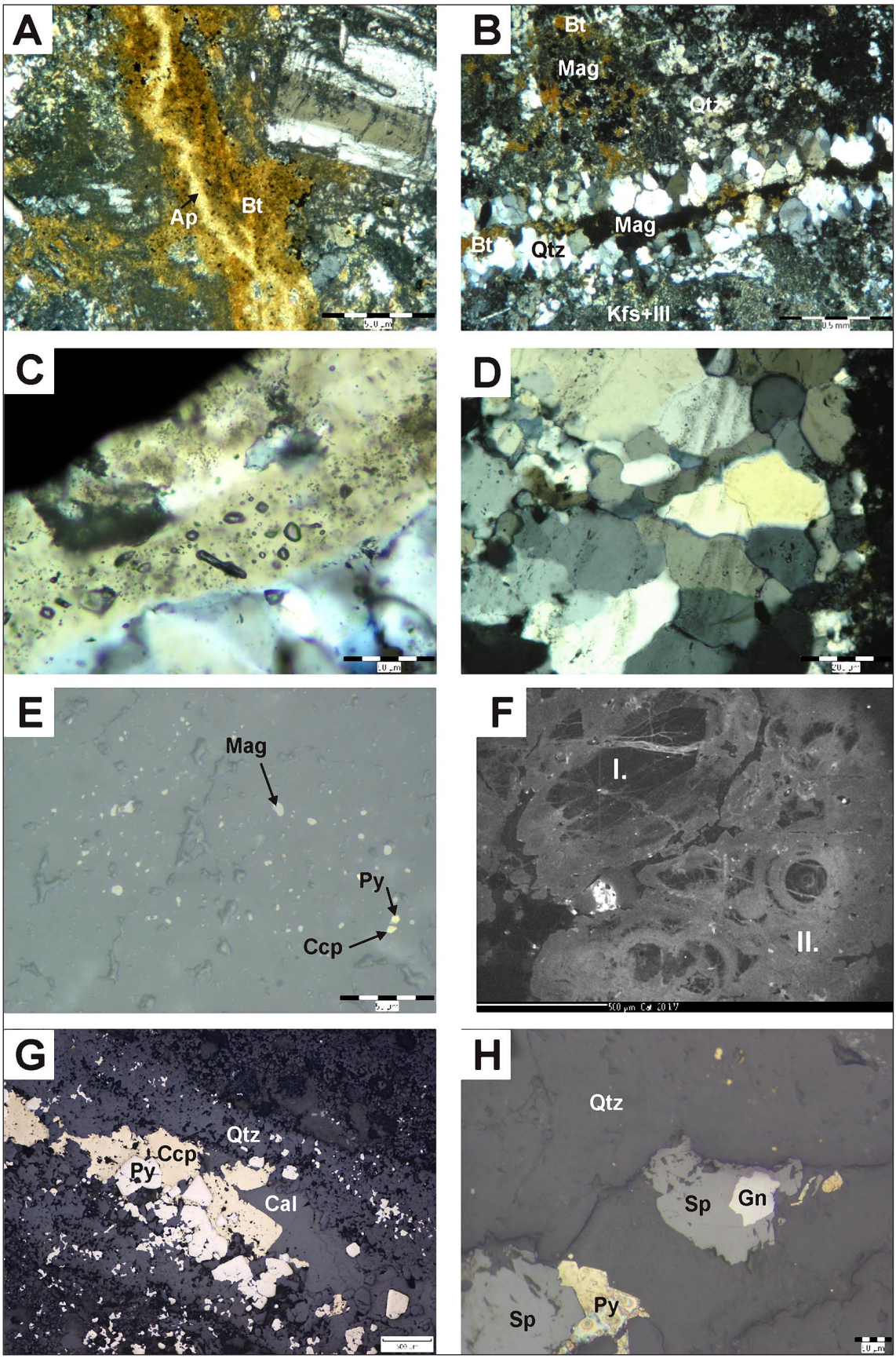

Fig. 12. Microphotographs of veinlets from the Biely vrch deposit. **A** – biotite-magnetite (EB-veinlet) with later stage apatite in its central part (DVE-5a/42.5; XN); **B** – quartz-biotite-magnetite veinlet (A-type) in porphyry affected by K-silicate alteration (DVE-1/72.6 m, XN); **C** – banded quartz veinlet with a band rich in vapour monophase type of inclusions (DVE-5a/369.6; XN); **D** – detail of bands of vapor-rich inclusions that do not respect quartz grains boundaries in a quartz veinlet (DVE-5a/417.6; XN); **E** – inclusion of magnetite and rare pyrite and chalcopyrite disseminated in quartz veinlets (DVE-5a/495.5; reflected light); **F** – cathodoluminiscence image of a thick cluster of hydrothermal quartz from Fig. 11B. Note the presence of two different generations of quartz, early nonluminiscent crystals probably of metamorphic hydrothermal origin (I.) and late quartz with strong luminiscence and preserved colomorph texture (II.) (DVE-5a/104.6); **G** – pyrite, younger chalcopyrite and calcite filling central part of a quartz veinlet (DVE-11/394.7; reflected light); **H** – galena enclosed in sphalerite and overgrown by pyrite or marcasite in a quartz veinlet (DVE-1/100.5; reflected light).

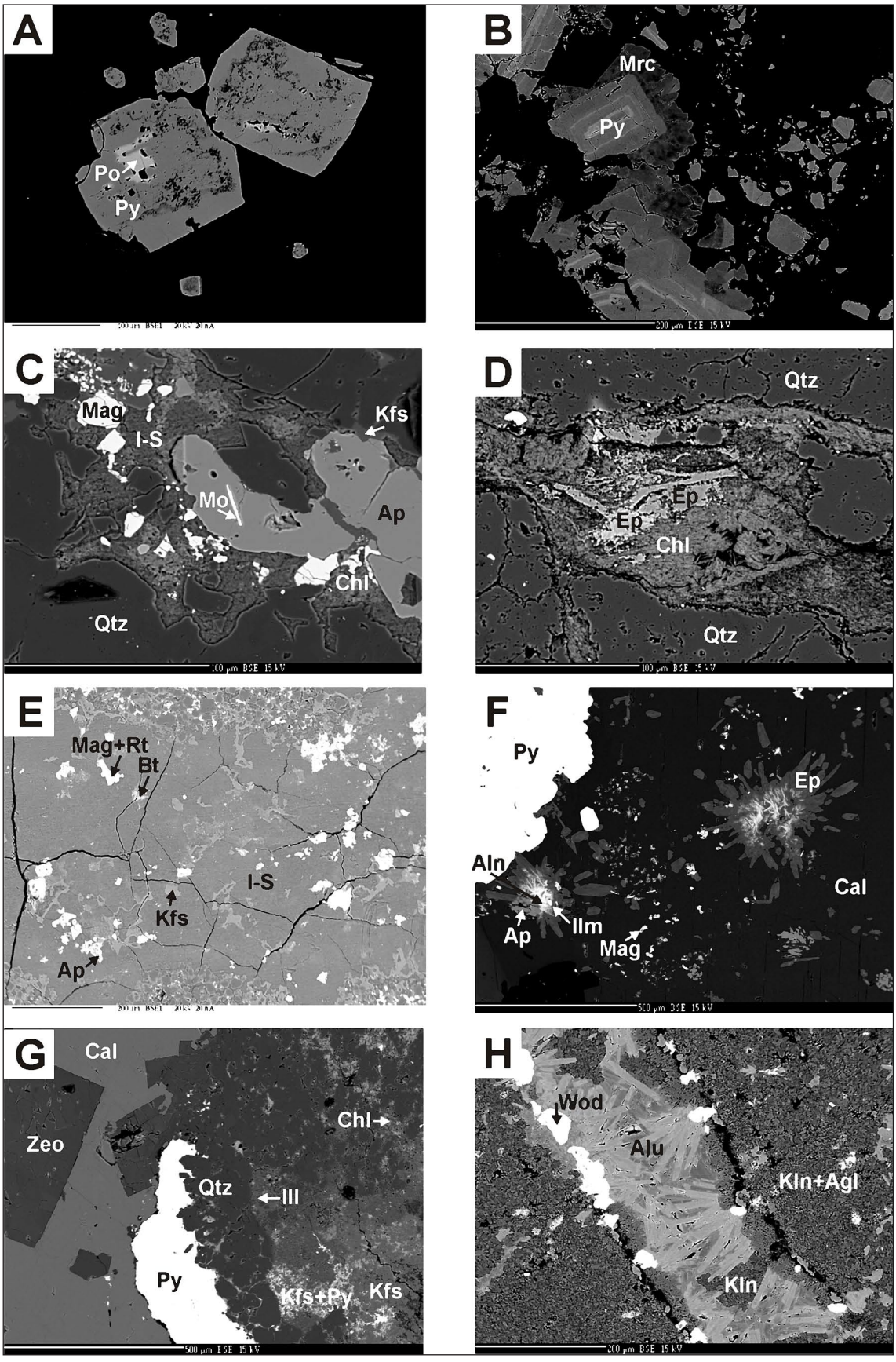

Fig. 13. Backscattered electron micrographs of mineralization in veinlets from the Biely vrch deposit. **A** – pyrite crystals enclosing pyrrhotite fragments (DVE-4/112.4); **B** – pyrite crystals overgrown by marcasite (DVE-5a/357.3); **C** – illite-smectite, chlorite, apatite, K-feldspar and magnetite filling central part of a quartz veinlet. Apatite encloses a tiny molybdenite crystal (DVE-3/163.0); **D** – chlorite with epidote filling central part of a quartz veinlet (DVE-5a/253.5); **E** – detail of intermediate argillic veinlet with dominant illite-smectite, enclosing biotite, K-feldspar, apatite, magnetite and rutile (DVE-4/66.4); **F** – calcite veinlet with pyrite clusters on its margins. Calcite hosts clusters of epidote with allanite in their centre and tiny magnetite and ilmenite grains (DVE-5a/310.7); **G** – complex vein filling with quartz overgrown by pyrite and later refilled by zeolite associated with calcite. Altered rock on the margin of the veinlet includes chlorite, illite, K-feldspar and pyrite representing intermediate-argillic alteration (DVE-5a/357.3); **H** – advanced argillic veinlet filled by woodhousite, alunite and kaolinite in strongly altered rock with kaolinite and augelite (DVE-8a/129.0).

gold at the deposit; however, vein quartz contains gold grains only rarely. Alteration halo in their vicinity is not always present, but sometimes silicification and increased amount of intermediate argillic alteration minerals have been observed (Figs. 7A, 8E and 11C).

Hydrothermal quartz also rarely occurs in big clusters, several centimeters in diameter (Fig. 11B). According to optical and cathodoluminiscence study quartz the clusters consist of several generations of quartz, including big zonal quartz crystals, overgrown by younger generation of more fine-grained quartz grains. Remnants of former colomorph (botryoidal) quartz have been also recognized, now disintegrated and recrystallized (Fig. 12F). Rare carbonate with zeolite and marcasite are filling gaps and forming short veinlets in some quartz clusters. The origin of quartz clusters is still not entirely understood, but probably the cores of the quartz grains represent metamorphic hydrothermal quartz enclosed as xenoliths in the porphyry and later overgrown by porphyry-related hydrothermal quartz, found elsewhere in veinlets. This interpretation is indicated by the presence of big blocks of Hercynian crystalline basement that were discovered by some drill holes at the deposit (Hanes et al., 2010).

Pyrite (sulphide) veinlets

Stand-alone sulphide veinlets are usually thin (<0.1 mm), short and discontinuous, with pyrite as the most common sulphide mineral. Pyrite-bearing veinlets are always younger than quartz veinlets, but are older than carbonate-zeolite veinlets. The same generation of sulphides also occurs in bands and clusters in the central part of quartz veinlets, while the clusters are up to 1 mm thick, probably filling former cavities in the veinlets (Figs. 12G and 12H). Less frequently, sulphides are also present in carbonate-zeolite veinlets or in clay veinlets (Figs. 13F and 13G).

Pyrite is variably accompanied by other sulphides, mostly chalcopyrite, galena, sphalerite, marcasite and rare tetrahedrite. Infrequent galena and sphalerite are often earlier than pyrite (Fig. 12H), while common chalcopyrite is always younger than pyrite (Fig. 12G). Tetrahedrite was found representing the single tiny inclusion in chalcopyrite. Marcasite is also a common but the youngest sulphide mineral, replacing earlier sulphides (Fig. 13B). Magnetite, Fe/Ti oxides and rare pyrrhotite are also sometimes present (Fig. 13A and 13F); however, they are always older than pyrite.

The pyrite-bearing veinlets in porphyry deposits usually associate with sericite alteration and are known as D-type veins (c.f. Gustafson and Hunt, 1975). However, within the studied samples from the Biely vrch locality, no association of pyrite veinlets with sericite alteration has been observed, thus they probably can not be classified as the D-veins. Their common association with the base metal minerals and clay minerals more likely indicates affiliation to intermediate-argillic alteration and/or propylitic alteration in marginal parts of the system (Seedorf et al., 2005).

Chlorite/intermediate argillic veinlets

Despite the widespread presence of chloritic and intermediate argillic alteration at the Biely vrch deposit, these alteration minerals only rarely form individual veinlets. If present, they are short, discontinuous, 1 mm to 0.1 mm thick and younger than quartz veinlets (Fig. 11E). Bands or clusters dominated by these minerals can be also found in quartz veinlets, mostly in their central parts (Fig. 13C and 13D).

There is not a clear difference between the chlorite and intermediate argillic veinlets (illite to illite-smectite) and sometimes both minerals occur together and appear to be coeval (Fig. 13C). However, chlorite-dominated veinlets are often accompanied variably by epidote (often REE-enriched), magnetite, sulphides (mainly pyrite and chalcopyrite) and overprinted by zeolite and calcite (Fig. 13D). Clay-dominated veinlets are variably accompanied by apatite, magnetite, rutile, K-feldspar and sulphides (Fig. 13E). Rare presence of micrometer-sized sphalerite, molybdenite, tourmaline, xenotime, allanite has been also observed. Rare solitary molybdenite also occurs within the late fissures (Fig. 13C).

Calcite-zeolite veinlets

This type of veinlets is relatively common, except of areas affected by advanced argillic alteration. Carbonate--zeolite veinlets are of variable thickness reaching often up to 1 cm, but common are also veinlets just 10 μm thin. They occur as individual veinlets cutting all other types of veinlets (Fig. 11G) except of advanced argillic ones.

Carbonate was identified as calcite and it is the most common mineral in these veinlets. Very often calcite is accompanied by various zeolite minerals (Fig. 13G) that rarely also form monomineral veinlets. Calcite-dominated veinlets also contain variably chlorite, epidote, K-feldspar, apatite, illite-smectite, pyrite, marcasite, magnetite, titanite, rutile, tourmaline, alanite on their margins and are clearly older than both calcite and zeolites (Fig. 13F). Zeolites are always older than calcite (Fig. 13G).

Carbonate-zeolite veinlets never occur in contact with advanced argillic veinlets, thus their mutual relationship is unclear. However, calcite veinlets are probably older, missing in areas of advanced argillic alteration due to leaching by corresponding low pH fluids. Carbonate-zeolite veinlets represent late, low-temperature veins related to final stages of porphyry systems (Seedorf et al., 2005).

Advanced argillic veinlets

In places affected by advanced argillic alteration veinlets with corresponding minerals are frequently present. They are always younger than quartz veinlets (Fig. 11F) and younger than intermediate argillic and pyrite veinlets (based on the succession of alteration discussed above).

Most common are veinlets with kaolinite and/or pyrophyllite. They are up to 2 mm thick, accompanied by broad alteration haloes with kaolinite (Fig. 11F). Veinlets are either nearly monomineral or represent mixtures of both

clays, accompanied variably by alunite, woodhousite and augelite that sometimes occur on margins of clay veinlets (Fig. 13H). Woodhousite is always the oldest in the mineral assemblage, but alunite is the most common. Locally, kaolinite veinlets also contain dickite, pyrite and rutile.

Gold mineralization

The extent of Au mineralization at the Biely vrch deposit roughly corresponds to the extent of quartz veinlets (Fig. 14). Grains visible in optical microscope we were able

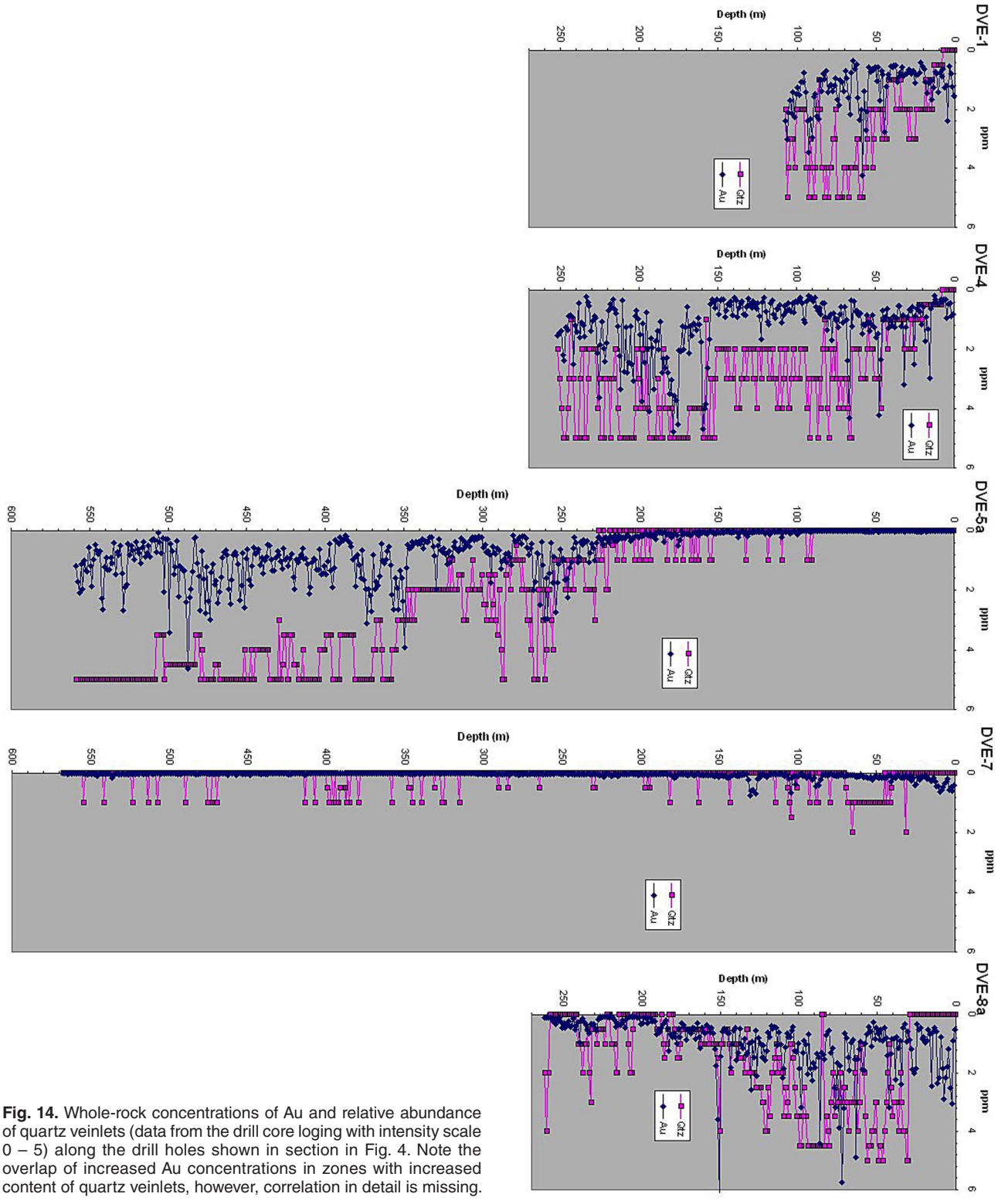

Fig. 14. Whole-rock concentrations of Au and relative abundance of quartz veinlets (data from the drill core loging with intensity scale 0 – 5) along the drill holes shown in section in Fig. 4. Note the overlap of increased Au concentrations in zones with increased content of quartz veinlets, however, correlation in detail is missing.

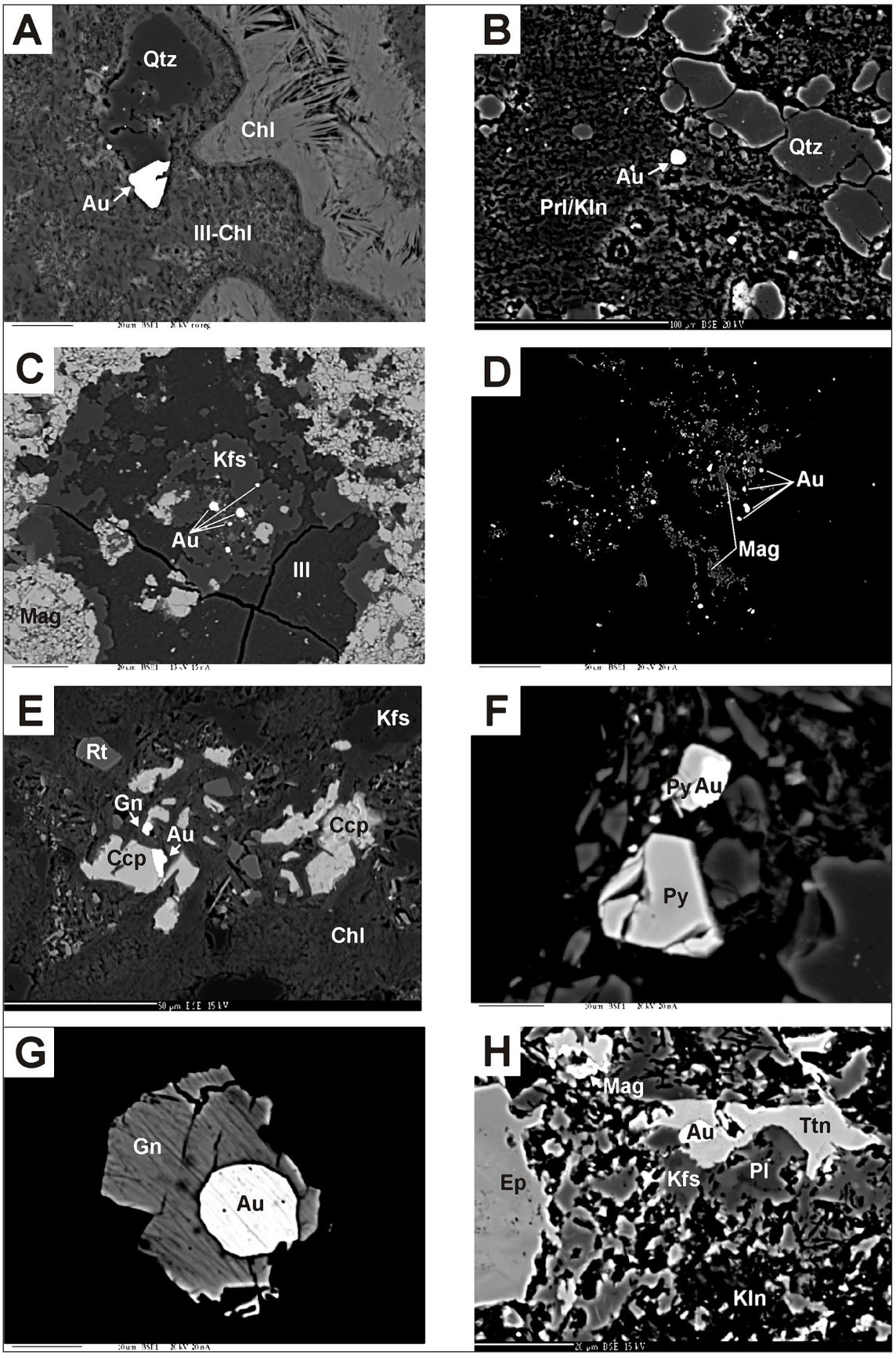

Fig. 15. Backscattered electron micrographs of Au mineralization from the Biely vrch deposit. **A** – gold grain attached to quartz in argillized rock with illite and chlorite close to a chlorite veinlet (DVE-5a/502.4); **B** – gold grain hosted by pyrophyllite/kaolinite in the vicinity of a small quartz veinlet (DVE-4/214.0); **C** – cluster of several small gold grains in illite associated with K-feldspar and magnetite (DVE-1/58.5); **D** – numerous tiny gold grains associated with magnetite in argillized rock with illite-smectite and kaolinite (DVE 4/188.6); **E** – gold grain attached to chalcopyrite and associated with rutile and galena hosted by altered rock with chlorite and K-feldspar (DVE-5a/349.5); **F** – gold grain enclosed in pyrite in silicified rock with illite-smectite (DVE-1/106.5); **G** – large isometric gold grain enclosed in galena (DVE-1/106.5); **H** – gold grain enclosed in titanite in altered rock with K-feldspar, kaolinite, epidote, plagioclase and magnetite (DVE-5a/478.2).

Tab. 2
Representative WDS analyses of gold from the Biely vrch deposit

Anal. No.	1	2	3	4	5	6	7	8	9
Hole	DV-1/100.5	DVE-1/106.5	DVE-4/66.4	DVE-4/188.6	DVE-4/206.7	DVE-5A/487.7	DVE-5A/487.7	DVE-5A/529.0	DVE-8A/72.5
Au	88.28	96.13	93.11	85.90	99.29	95.85	98.39	98.47	97.49
Ag	12.59	3.41	7.73	12.36	0.15	3.97	2.69	2.11	0.57
Cu	0.03	0.05	0.09	0.02	0.04	0.02	0.03	0.06	0.00
Hg	0.00	0.28	0.05	0.00	0.00	0.08	0.16	0.03	0.05
Total	100.90	99.86	100.98	98.28	99.48	99.92	101.26	100.66	98.10

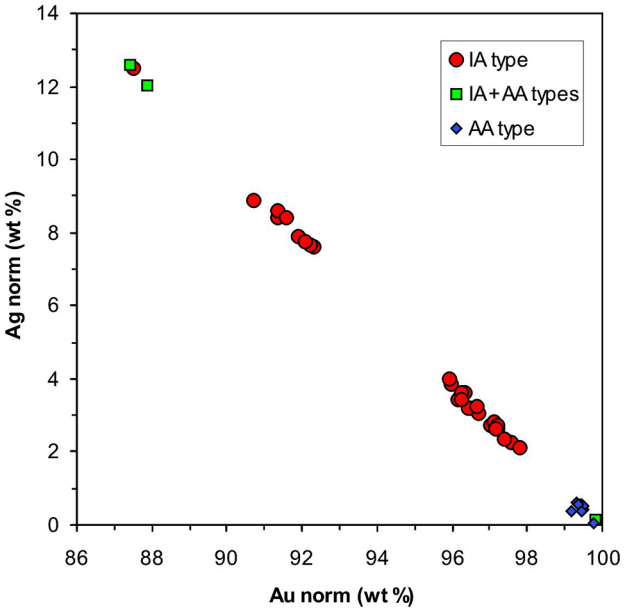

Fig. 16. Correlation between normalized Au and Ag concentrations of gold grains from the Biely vrch deposit based on microprobe data. Grains are hosted either by intermediate argillic (IA) or advanced argillic (AA) alteration mineral assemblages or a mixture of both (IA + AA).

to find only where gold grades were > 0.5 g/t. The grain size of gold is variable, generally 2 – 15 μm in diameter, rarely up to 40 μm. However, significant proportion of gold is probably also distributed in the form of submicroscopic grains (< 2 μm) as seen in detailed SEM images (Figs. 15C and 15D) and preliminary LA ICPMS work.

Most of the observed gold grains are not hosted by quartz veinlets, but they occur in their broad vicinity within altered rock variably associated with clays (illite, illite/smectite, kaolinite), chlorite, K-feldspar, plagioclase, epidote, zeolite (Figs. 15A, 15C, 15E and 15H). Sometimes some ore minerals are also associated, usually chalcopyrite, magnetite, pyrite and rutile (Figs. 15D and 15E). Rarely gold is directly attached to pyrite, chalcopyrite or included in galena, titanite, rutile (Figs. 15E and 15H). As the gold is not generally present in veinlets there is not a direct correlation between the gold grades and the amount of quartz veinlets, neither with the presence of particular generation of quartz veinlets (e.g. banded or not banded, Fig. 14).

The microprobe analyses of 28 individual gold grains (42 analyses in total) showed that most of the gold grains are very pure, homogeneous, with small but variable concentrations of Ag (0.05 to 12.6 wt.%; Tab. 2). Correlation between normalised Au and Ag contents of gold shows three distinct clusters of Au/Ag ratios, probably indicating the presence of multiple generations of gold at the deposit (Fig. 16). Other components (Hg and Cu) are present just in the very small concentrations (Hg < 0.4 wt.%, Cu < 0.3 wt.%). Gold in zones overprinted by advanced argillic alteration shows generally higher fineness (992 to 994 with the exception of one sample) compared to gold in rocks affected by intermediate argillic alteration only (875 – 978). This can be interpreted as the result of remobilization of gold by these late stage fluids, resulting in loss of Ag. Furthermore, gold grains hosted by kaolinite are sometimes accompanied by the dense clusters of tiny (< 2 μm) gold grains which might indicate the local dissolution and quick

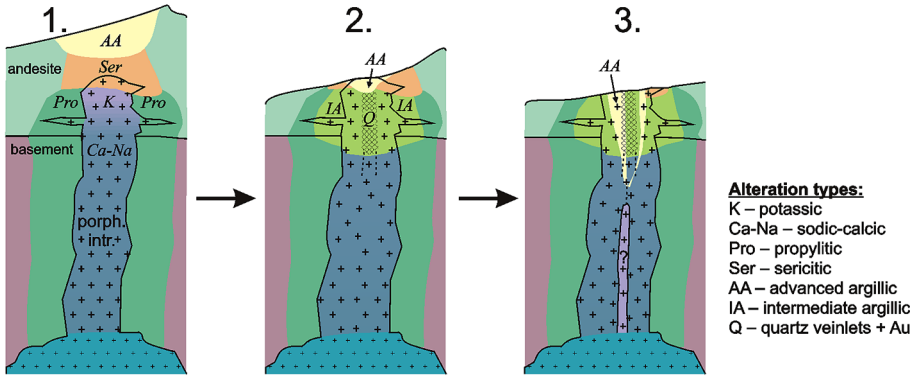

Fig. 17. Schematic model showing succession of alteration patterns at the Biely vrch Au-porphyry deposit, assuming a shallow emplacement of the parental intrusion (not to scale). See text for arguments defending the model.

reprecipitation of gold due to neutralization at wall rocks, which corresponds to a very low ability of acid fluids to transport Au complexes (Heinrich, 2005).

Discussion

Detailed study of alterations and mineral assemblages of the Biely vrch deposit further confirmed the classification of the deposit as a typical Au-porphyry deposit. Compared to other Au-porphyry systems worldwide, in addition to low Cu/Au ratio and association with diorite porphyry intrusions it also shares some other specific features. They include enrichment in magnetite, the presence of banded quartz veinlets with vapour-rich inclusions and the occurrence of related advanced argillic alteration (Muntean and Einaudi, 2000; Sillitoe, 2000; Seedorf et al., 2005).

The sequence of alteration patterns determined in this study enables to reconstruct the possible evolution of this magmatic-hydrothermal system (Fig. 17). First stage of evolution includes emplacement of the parental porphyry intrusion and alteration patterns developed by the early high temperature fluids (K alteration in upper parts, Ca--Na alteration in deeper parts). In agreement with porphyry systems evolution models, there is highly probable the simultaneous evolution of lithocap with advanced argillic alteration close to the surface due to condensation of magmatic gases rich in acid-forming components (mainly SO_2). The presence of transitional quartz-sericite-pyrite (phyllic) alteration is also assumed below the lithocap.

Second stage of evolution is marked by the development of network of quartz veinlets, probably associated with input of the main portion of magmatic fluids exsolved from the underlying magma chamber into the partially cooled intrusive body. Shallow emplacement of the veinlets corresponds to the observed presence of banded and botryoidal textures, resulting from local crystallization from the silica gel, induced probably by rapid fluid decompression and cooling (Fournier, 1985). Note, that at this time some paleosurface degradation is assumed of the soft argillized material, which enabled the observed high degree of telescoping of younger alteration over older ones. Widespread intermediate argillic alteration, that is also supposed to have originated during this stage, is overprinted on K and Ca-Na alterations down to the lowest explored parts of the deposit (~400 m). Precipitation of IA alteration is related to nearly neutral pH fluids, linked to progressive cooling of the system with initial meteoric water incursion (Sillitoe, 2002) and/or influx of late-stage, low temperature, low salinity magmatic fluid (Hedenquist et al., 1998). Despite the fact that quartz veinlets sometimes have a clear alteration halo of IA type, it is still not clear if the widespread IA type of alteration is coeval or postdates the emplacement of veinlets. High degree of telescoping and evidence of quick decompression within quartz veinlets enables to speculate even about a possible gravitationally induced catastrophic sector-collapse of volcanic edifice and sudden removal of overbunded, which is suggested to explain these features on Au-porphyry deposits (Sillitoe, 2000).

Third stage of the model corresponds to the origin of zones and ledges of advanced argillic alteration that generally result from condensation of magmatic vapour enriched in acidic volatiles. These fluids are likely related to a new portion of magma emplaced at depth, that experienced strong structural fluid focusing at fluid--dominated conditions.

Distribution of gold shows spatial association of Au mineralization with the presence of quartz veinlets. However, the quartz veinlets themselves rarely host gold grains and gold occurs in altered rock in their vicinity. Thus, it is likely that most of the gold was introduced into the system during the emplacement of quartz veinlets due to reaction with the favourably altered surrounding rock. The associated low density fluid inclusions indicate transport of Au in bisulfide complexes. Their efficient destabilization (leading to gold precipitation) was probably induced by focusing of Au-bearing fluids into favourably altered rocks (potassic) with enough feldspar for effective H^+ sink and enough Fe-oxides for effective de-sulfidation of the fluid by iron in the wall rocks rich in magnetite (Heinrich, 2005). Furthermore, rapid depressurization indicated by the presence of botryoidal quartz and large--scale telescoping could have steepened the gradients of chemical disequilibrium and quick destabilization of Au--complexes. The associated low-density vapour-like fluid probably results from brine-vapour fluid phase separation deeper in the system, while Au partitioned strongly into the vapour phase (Williams-Jones and Heinrich, 2005).

In detail, however, the history of gold precipitation is most likely more complicated as suggested by several generation of gold with different fineness (Fig. 16). Some of the gold might have been already introduced together with potassic alteration as suggested by Sillitoe (2000) for genesis of Au in Au-rich porphyry systems. For instance, at the Cerro Casale Au-rich deposit gold deposited during potassic alteration has high abundances of Ag (8 – 28 wt.% Ag), but gold deposited during intermediate argillic alteration has much lower Ag content (1 – 9 wt.% Ag). If the same feature is applied on the Biely vrch Au data, most of the gold was clearly precipitated during the intermediate argillic alteration stage. Furthermore, apparent gold enrichment in zones of advanced argillic alteration overprinting quartz veinlet stockwork indicates remobilization of gold. This corresponds to a very high fineness of this gold, related to loss of Ag during the process of remobilization. As elsewhere at Biely vrch and most other localities within the Javorie stratovolcano the AA type of alteration is barren (Hanes et al., 2010), introduction of primary Au during the third stage of evolution is highly unlikely.

Conclusions

The Biely vrch deposit is a typical Au-porphyry system, sharing all major characteristics of this type of porphyry deposits, but it was not known previously in the Central Slovakian Volcanic Field. Within the identified types of alterations the intermediate argillic alteration clearly dominates, variably overprinting earlier high-temperature

K-silicate and Ca-Na silicate alterations in deeper levels of the magmatic-hydrothermal system. Chloritic alteration appears locally as transitional stage between K-silicate and IA alteration stages. Propylitic alteration represents an outer zone of the system. Crosscutting subvertical ledges of advanced argillic alteration correspond to the youngest stage of hypogene alteration, probably related to a younger intrusive event. Alterations are accompanied by corresponding veinlets, including early EB- and A-types, widespread quartz, younger pyrite and IA/chloritic and final zeolite-carbonate and AA veinlets.

Quartz veinlets mark the area of economic Au mineralization and are supposed to be associated with input of magmatic fluids exsolved from the underlying magma chamber up to shallow levels of the system and influenced by a quick decompression. Low density fluids entered into the partially cooled intrusive body during or prior to the origin of IA alteration. Gold of microscopic to submicroscopic size is present in the vicinity of quartz veinlets in altered rock typically with clays, chlorite, K-feldspar and Fe-Ti oxides, and is sometimes attached to sulphide minerals. Most of the gold was introduced into the system in bisulphide complexes in vapor during the emplacement of quartz veinlets and precipitated due to reaction of fluid with K-feldspars (effective H^+ sink) and Fe-oxides (effective for de-sulphidation of the fluid) in the regime of fluid decompression. Several generations of gold with variable fineness point to multiphase introduction of gold into the system and significant role of its remobilization especially during penetration of fluids responsible for advanced argillic alteration.

Acknowledgements. Support by EMED Mining, Ltd. and VEGA grant 1/0311/08 is acknowledged.

References

Burian, J. & Smolka, J., 1982: Geology of the porphyry copper deposit Zlatno. *In: Miner. Slov. (Bratislava), 14, 517 – 538 (In Slovak).*

Fournier, R. O., 1985: The behaviour of silica in hydrothermal solutions. *In: Rev. Econ. Geol., v. 2, 45 – 60.*

Gustafson, L. B. & Hunt, J. P., 1975: The porphyry copper deposit at El Salvador, Chile. *In: Econ. Geol. (New Haven), 70, 857 – 912.*

Gustafson, L. B. & Quiroga, G., 1995: Patterns of mineralization and alteration below the porphyry copper orebody at El Salvador, Chile. *In: Econ. Geol. (New Haven), 90, 2 – 16.*

Hanes, R., Bakos, F., Fuchs, P., Žitňan, P. & Konečný, V., 2010: Exploration results of Au porphyry mineralization in the Javorie stratovolcano. *In: Miner. Slov. (Bratislava), 42, 15 – 32.*

Heinrich, C. A., 2005: The physical and chemical evolution of low-salinity magmatic fluids at the porphyry to epithermal transition: A thermodynamic study. *In: Mineralium Deposita, 39, 864 – 889.*

Hedenquist, J. W., Arribas, A., Jr. & Reynolds, T. J., 1998: Evolution of an intrusion-centred hydrothermal system: Far Southeast--Lepanto porphyry and epithermal Cu-Au deposits, Philippines. *In: Econ. Geol. (New Haven), 93, 373 – 404.*

Konečný, V., Mihaliková, A. & Rojkovičová, L., 1977: Structural drill hole KON-1. Open file report. *Manuscript. Bratislava, archive State Geol. Inst. D. Štúr, 185 (In Slovak).*

Konečný, V., Miko, O., Straka, P., Panáček, A. & Šefara, J., 1988: Geological structure and morphostructures of basement of the eastern part of the Central Slovakian Volcanic Field (Krupinská planina – Zvolen) at a scale 1 : 100 000. Open file report. *Manuscript. Bratislava, archive State Geol. Inst. D. Štúr (In Slovak).*

Konečný, V., Lexa, J., Halouzka, R., Hók, J., Vozár, J., Dublan, L., Nagy, A., Šimon, L., Havrila, M., Ivanička, J., Hojstričová, V., Mihaliková, A., Vozárová, A., Konečný, P., Kováčiková, M., Filo, M., Marcin, D., Klukanová, A., Liščák, P. & Žáková, E., 1998: Explanations to the geological map of the Štiavnické vrchy and Považský Inovec mountain ranges (Štiavnica stratovolcano). *Bratislava, GS SR, 473 (In Slovak with English summary).*

Konečný, V., Lexa, J. & Žáková, E., 2002: Hydrothermal center Biely Vrch near Detva. Partial final report. *In: Lexa, J. et al., 2002: Metallogenetic evaluation of the territory of Slovak Republic. Open file report. Manuscript. Bratislava, archive State Geol. Inst. D. Štúr (In Slovak).*

Marsina, K., Lexa, J., Rojkovičová, Ľ., Konečný, V., Žáková, E., Hojstričová, V., Konečný, P. & Káčer, Š., 1995: Comparison of porphyry/skarn objects in the central zone of the Štiavnica stratovolcano and their resource assessment. Open file report. *Manuscript. Bratislava, archive State Geol. Inst. D. Štúr, 119 (In Slovak).*

Mihaliková, K., 1985: Structural drill hole DV-24, Zltý Vŕšok, Poľana. Unpublished graduation thesis. *Bratislava, Archive Fac. Nat. Sci. Comenius Univ. (In Slovak).*

Muntean, J. L. & Einaudi, M. T., 2000: Porphyry gold deposits of the Refugio district, Maricunga belt, northern Chile. *In: Econ. Geol. (New Haven), 95, 1 445 – 1 472.*

Muntean, J. L. & Einaudi, M. T., 2001: Porphyry-epithermal transition: Maricunga belt, northern Chile. *In: Econ. Geol. (New Haven), 96, 743 – 772.*

Ramdohr, P., 1980: The ore minerals and their intergrowths. Second edition. *New York, Pergamon, 1 207.*

Seedorff, E., Dilles, J. H., Phoffett, Jr., J. M., Einaudi, M. T., Zurcher, L., Stavast, W. J. A., Johnson, D. A. & Barton, M. D., 2005: Porphyry deposits: Characteristics and origin of hypogene features. *Littleton, Economic Geology 100th Anniv. Vol., Soc. Econ. Geol., 251 – 298.*

Sillitoe, R. H., 2000: Gold-rich porphyry deposits? Descriptive and genetic models and their role in exploration and discovery. *In: Hagemann, S. G. & Brown, P. E. (eds.): Gold in 2000. Rev. Econ. Geol., 13, 315 – 315.*

Štohl, J., Konečný, V., Mihaliková, A., Žáková, E., Marková, M. & Rojkovičová, L., 1981: Metallogenetic exploration of Javorie. Open file report. *Manuscript. Bratislava, archive State Geol. Inst. D. Štúr (In Slovak).*

Štohl, J., Dublan, L., Hojstričová, V., Marková, M., Marsina, K., Mihaliková, A., Mihaliková, K., Onačila, D., Stankovič, J. & Žáková, E., 1986: Evaluation of possible Cu (Pb-Zn) ore mineralization in the area of Javorie (Štožok – Klokoč) and Poľana. Open file report. *Manuscript. Bratislava, archive State Geol. Inst. D. Štúr (In Slovak).*

Vasyukova, O. V., Kamenetsky, V. S. & Gömann, K., 2008: Origin of "quartz eyes" and fluid inclusions in mineralized porphyries. *In: Geochim. Cosmochim. Acta (Oxford), 72, Suppl. 1, p. A978.*

Vila, T. & Sillitoe, R. H., 1991a: Gold-rich porphyry systems in the Maricunga belt, Northern Chile. *In: Econ. Geol. (New Haven), 86, 1 238 – 1 260.*

Williams-Jones, A. E. & Heinrich, C. A., 2005: Vapor transport of metals and the formation of magmatic-hydrothermal ore deposits. *In: Econ. Geol. (New Haven), 100, 1 287 – 1 312.*

Rukopis doručený 1. 2. 2010
Revidovaná verzia doručená 12. 2. 2010
Rukopis akceptovaný red. radou 17. 2. 2010